

Axial buckling design equation for
thermoplastic lined carbon steel



Axial buckling design equation for thermoplastic lined carbon steel

by

L.M. de Mul

RESTRICTED

This document is made available subject to the condition that the recipient will neither use nor disclose the contents except as agreed in writing with the copyright owner. Copyright is vested in Shell Global Solutions International B.V., The Hague.

© Shell Global Solutions International B.V., 2009. All rights reserved.

Neither the whole nor any part of this document may be reproduced or distributed in any form or by any means (electronic, mechanical, reprographic, recording or otherwise) without the prior written consent of the copyright owner.

Shell Global Solutions is a trading style used by a network of technology companies of the Shell Group.

Summary

Thermoplastic lined pipelines are successfully used within the oil and gas industry to prevent corrosion of carbon steel pipelines and flowlines. The application of thermoplastic lined carbon steel is currently often limited by the maximum allowable operating temperature of the polymer. For e.g. HDPE this is set to 60 °C and for PA-11 at 65 to 85 °C.

From operating experience with HDPE lined pipe within the current temperature window, up to 60 °C, it was found that radial collapse is the dominating mechanism. Only a few failures where axial collapse has occurred have been reported. These failures occurred in liners with a low wall thickness in combination with either a high operating temperatures, higher than 90 °C thus exceeding by far the allowable current design limit of 60 °C, or significant levels of swell. An increase of the maximum operating temperature is expected to increase the probability for axial collapse. Liners, therefore, have to be designed to be axial collapse resistant.

In the present study, an axial liner collapse model was developed and validated by testing and finite element calculations.

Amsterdam, December 2009

Table of contents

Summary	1
1. Introduction	3
2. Scope of work	4
2.1 Task 1: finite element analysis	4
2.2 Task 2: axial buckling experiments	4
2.2.1 Small scale experiments	4
2.3 Development of an engineering equation to predict axial collapse	4
3. Axial buckling and collapse	4
3.1 Axial buckling and collapse experiments	4
3.1.1 Test set-up	4
3.1.2 Radial imperfections	6
3.1.3 Liner specimens	7
3.1.4 Experiments and results	8
3.1.4.1 Temperature dependency	8
3.1.4.2 Strain rate dependency	9
3.1.4.3 Determination imperfection size dependency	10
3.1.4.4 Determination SDR dependency	11
3.1.5 Axial buckling and collapse modelling using finite element analysis	13
3.1.5.1 Critical strain calculations	14
3.1.5.2 Correction for friction	14
3.1.5.3 Correction for lobe deformation	15
3.1.5.4 Correction for pin support	17
3.1.5.5 Overall displacement correction	17
3.2 Axial collapse equation	18
3.3 Acceptance criterion for axial strain	21
3.3.1 Axial strain in liner during service	21
3.3.2 Field factors	22
3.3.2.1 Friction	22
3.3.2.2 Pre-tensioning	22
3.3.3 Imperfection size	22
3.3.4 Flanges	23
3.3.5 Field experience axial failure	23
3.4 Required material properties for axial buckling calculations	24
3.5 Water service with low concentration of crude oil	25
3.6 Polyamide PA-12 versus HDPE	25
4. Discussion of results	25
5. Conclusions	25
6. Recommendations	25
7. References	26
Appendix A. Results F.E.A. Ruben van Schalkwijk	27
Appendix B. Alternative approach for axial collapse equation based on maximum push load calculation method	45
Appendix C. Derivation of linear swell from volumetric swell	46
Appendix D. Data PA-12 (source Evonik-Degussa)	48
Bibliographic information	51
Report distribution	52

1. Introduction

Thermoplastic lined pipelines, mainly lined with High-density polyethylene (HDPE) and to a lesser extent polyamide (PA-11), are successfully used by the Shell Operating Units to prevent corrosion of carbon steel pipelines and flowlines. The main advantage of polymer liners is their inherent corrosion resistance and the relatively low cost of the material. The total installed cost of e.g. a HDPE lined carbon steel pipe is typically a factor of 2 to 3 lower than a conventional corrosion resistant alloy pipe. With the steep increase of the price of corrosion resistant alloys, over the last years, the availability of alternative pipe systems has become more important.

The application of thermoplastic lined carbon steel is currently often limited by the required operating temperature. This limit for HDPE is set to 50 °C to 60°C and for PA-11 to 65 °C to 80 °C depending on the type of service. This temperature limit originates from typical stress limitations of HDPE and PA-11 stand-alone pipes.

Based on the present expertise and operating experience [1,2,3], the temperature limit of HDPE liners is primarily determined by the reduction in stiffness. The uptake of service fluids, such as hydrocarbons, may result in an additional reduction in stiffness, but in most cases this effect is much smaller than the temperature effect.

Prevention of liner buckling and collapse, radial or axial, is one of the key design issues in liner design. As long as the stiffness of the liner is sufficient to provide the required collapse resistance at the design temperature, it should be possible to extend the design temperature window to a higher temperature.

Historically, the wall thickness of a liner system was designed against radial collapse only. From operating experience within the current temperature window, up to 60 °C, it was found that radial collapse was the dominating failure mechanism.

To mitigate the probability for axial collapse, liner pre-tensioning is applied during installation to handle the axial extension of the liner as a result of the operating temperature and liner swell due to the uptake of service fluids. The combination of radial collapse design and pre-tensioning the liner has resulted in successful operation of liners over the last 20 years.

Only a few failures where axial collapse has occurred have been reported. These failures occurred in liners with a low wall thickness in combination with either a high operating temperatures, higher than 90 °C, thus exceeding by far the allowable current design limit of 60 °C, or significant levels of swell [3,4].

An increase of the maximum operating temperature is expected to increase the probability for axial collapse. Liners, therefore, have to be designed to be axial collapse resistant. Since no validated axial liner collapse models were available, a design method has been developed and validated by testing and finite element calculation.

The main objective of the present study was to develop a design engineering equation to predict the axial buckling as function of the temperature for a given liner diameter and liner thickness.

2. Scope of work

The following scope of work was agreed.

2.1 Task 1: finite element analysis

Finite element analyses were used to determine the axial force at which a liner with given geometry and materials properties will buckle in axial mode. The driving force for axial buckling is axial strain, caused by thermal expansion and swelling. Analysis performed using thermoplastic materials properties of HDPE and PA-12 in the range of 20 to 100 °C and liners in the range of 6" to 52". The results were used to compare the small-scale axial buckling experiments as described in Task 2.

2.2 Task 2: axial buckling experiments

2.2.1 Small scale experiments

Axial buckling experiments were performed on 6" liners to determine the axial force at which a liner with a given geometry and material properties would axial buckle.

The first phase of the experimental programme was carried out on a HDPE liner as it is currently used in one of Shells operating units in the Middle East.

The second phase of the experimental programme was carried out on the PA-12 material as delivered by Evonik Degussa. The axial collapse was measured on a 6" liner in a compression test set-up at 20, 40, 60, 80 and 100 °C. The force at which axial buckling occurred was determined.

Deliverable:

Buckling forces as a function of temperature and wall thickness, comparison with finite element analysis as described under Task 1.

2.3 Development of an engineering equation to predict axial collapse

The overall deliverable of the Tasks 1 and 2 is an engineering equation to predict the axial buckling as a function of stiffness.

3. Axial buckling and collapse

3.1 Axial buckling and collapse experiments

3.1.1 Test set-up

The axial buckling and collapse tests were performed on liner specimens installed inside a steel host pipe. A drawing of the test set-up is shown in Figure 1. A picture of a lined pipe specimen is shown in Figure 2.

The lined pipe specimens were placed on a steel support of a tensile testing machine. The lined pipe specimen could be moved in the vertical direction. On top of the liner specimen, a thick steel plate was placed with a diameter somewhat smaller than the inside diameter of the steel host pipe. This allowed movement inside the steel pipe without wall friction.

The steel plate was at a fixed position relative to the tensile test machine. The liner was loaded in axial compression moving the steel support of the tensile testing machine upward. Load and displacement were recorded. Displacement was continued until collapse of the liner occurred. Tests were performed in a temperature cabinet to enable testing at elevated temperatures. A picture of a lined pipe specimen inside the temperature cabinet is shown in Figure 3.

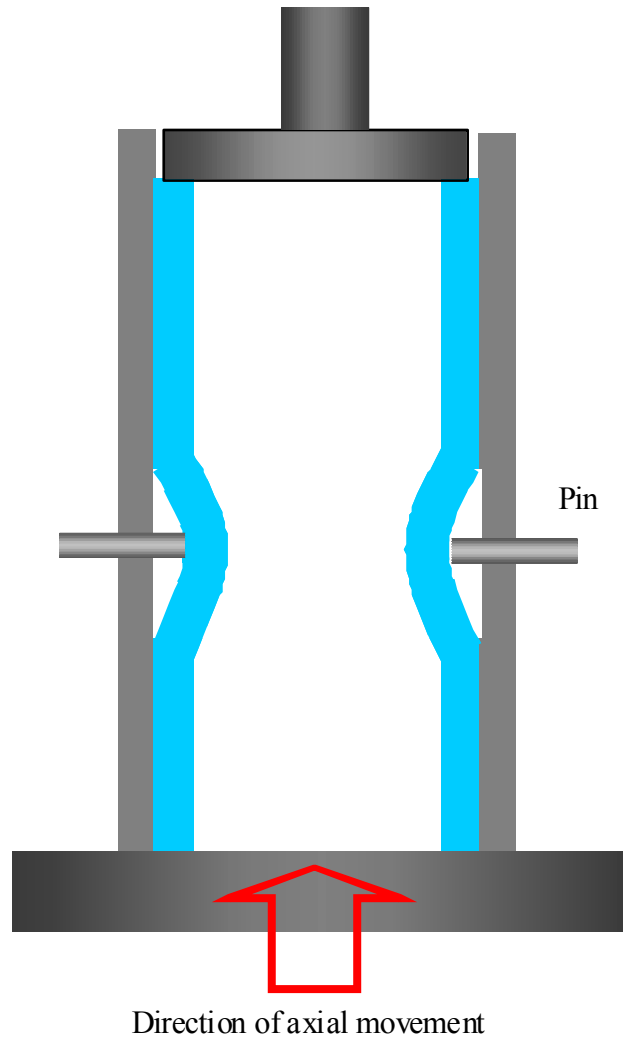


Figure 1 Test set-up



Figure 2 Lined pipe specimens, steel host pipe with HDPE liner, before the test



Figure 3 Lined pipe specimen during test inside temperature cabinet

3.1.2 Radial imperfections

A scouting test on a straight liner specimen did not result in buckling of the liner but plastic deformation of the top of the liner. It was concluded that the yield stress of the straight liner in compression was lower than the buckling stress. For a liner to buckle before yielding, therefore, a geometrical imperfection, such as an indentation is required in the liner.

Geometrical imperfections are local deformations of a liner caused, for example, by a protruding weld cap. The imperfection is given as the, Imperfection Over Diameter ratio (IOD), that is, the ratio of the imperfection size over the inner diameter of the host pipe, see Figure 4.

For a tight-fit liner, the internal diameter of the host pipe is identical to the outer diameter of the liner.

$$IOD = \frac{\Delta}{D} \quad (1)$$

Δ is the size of the imperfection [mm]

D is the inner diameter of the host pipe

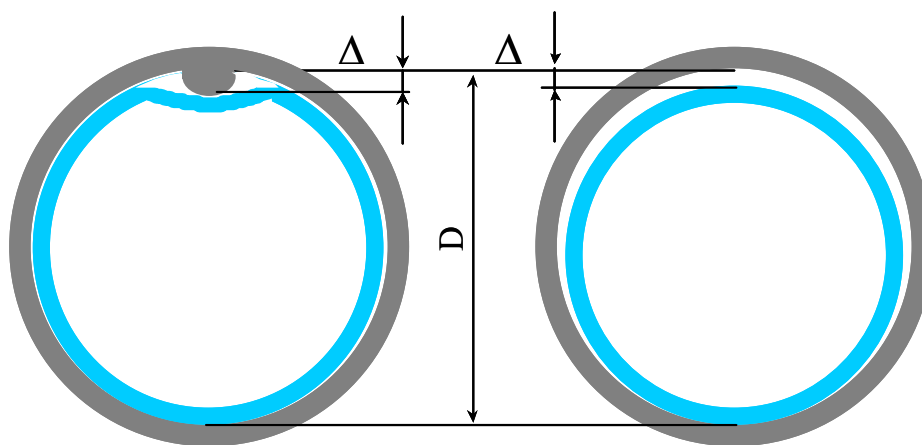


Figure 4 Liner imperfections, local deformation (left) and undersize (right)

To make such an imperfection in a controlled manner, threaded holes were machined into the steel host pipe in which screwing pins were installed, pressing the liner inward. The pins were located halfway along the length of the steel host pipe and the number of pins was such that the level of indentation was nearly constant along the liner circumference.

Figure 2 shows the arrangement of the screwing pins on the lined pipe specimen.

3.1.3 Liner specimens

Two different liner materials were tested, high-density polyethylene (HDPE) and polyamide 12 (PA-12).

The HDPE liner material is a typical HDPE grade as it is currently used within Shell. The properties of the HDPE material are provided in Table 1.

Table 1 HDPE properties

Property	HDPE
Density (gram/cc)	0.957 stdev = 0.001 (n = 15)
Maximum solubility coefficient n-Heptane (Mol/mm ³)	$9.44 \cdot 10^{-7}$ stdev = $9.3 \cdot 10^{-9}$ (n = 3)
Density after saturation (gram/cc)	0.921 (n = 3)
Volume change (%) to n-Heptane at 67 °C during about 91 hrs	13.7 stdev = 0.14 (n = 3)
Ultimate tensile strength (Mpa)	20.9 N = 1
Strain (UTS) (%)	10.6 n = 1
0.5 % Secant elasticity modulus (Mpa)	939 n = 1
5 % Secant elasticity modulus (Mpa)	385 n = 1

stdev = standard deviation

n = number of measurements

The PA-12 was provided Evonik-Degussa, specified as VESTAMID BS1170 (LX9020). The tensile curves of this material were provided by Evonik-Degussa (Appendix D).

Tests were performed on HDPE liners with a wall thickness of 8.5 mm and 9.9 mm. The PA-12 liners had a wall thickness of 5 mm.

The material and dimensions are listed in Table 2.

Table 2 Liner specimen material and dimensions

Material	OD (mm)	t (mm)	SDR	L (mm)
HDPE	193	8.5	22.7	320
HDPE	193	9.9	19.5	320
PA-12	75	5	15	180

3.1.4 Experiments and results

3.1.4.1 Temperature dependency

HDPE liner specimens with an SDR of 22.7 were tested at 20, 40, 60 and 80 °C. The liners were compressed until a deflection of 80 mm was reached; the deflection and resulting force were recorded. Table 3 shows the test parameters and critical deflections of HDPE liners. A plot of the results is shown in Figure 5.

Table 3 Test parameters and critical deflections of HDPE liners

Dimensions OD: 193 mm, t: 8.5 mm, L:320 mm

Test number	Temperature [°C]	Δ [mm]	IOD [%]	Strain rate [mm/min]	Critical deflection [mm]
1	20	2	1	0.035	22.6
2	40	2	1	0.035	23.6
3	60	2	1	0.035	22.9
4	80	2	1	0.035	19.4

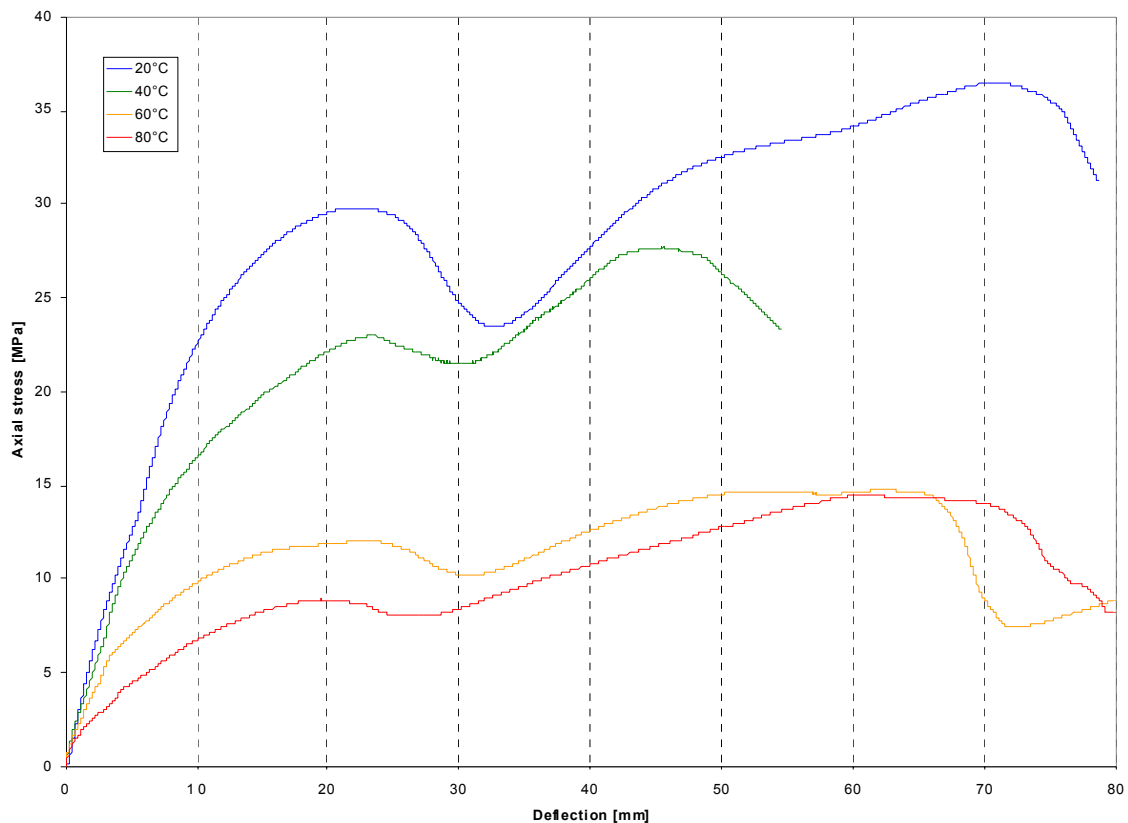


Figure 5

Axial compressive stress for HDPE as function of liner deflection at 20, 40, 60 and 80 °C

The results show an increase in stress until a deflection of approximately 22 mm. At this deformation, the buckling of the lobe becomes unstable, defined as the onset of collapse. Further deformation causes a decrease of the stress until further deformations of the lobe cause an increase in stress again.

Figure 6 shows a cross-section of an axial collapsed liner specimen.



Figure 6 A cross-section of an axial collapsed liner specimen (HDPE)

3.1.4.2 Strain rate dependency

HDPE liner specimens with a SDR of 19.5 were tested at three different strain rates: 5, 1 and 0.037 mm/min, to determine the strain rate dependency of the axial buckling phenomenon¹. Table 4 shows the test parameters and critical deflections of HDPE liners. A plot of the results is shown in Figure 7.

Table 4 Test parameters and critical deflections of HDPE liners

Dimensions OD: 193 mm, t: 9.9 mm, L:320 mm

Test number	Temperature [°C]	Δ [mm]	IOD [%]	Strain rate [mm/min]	Critical deflection [mm]
1	20	3.0	1.55	1	Not successful
2a	40	3.0	1.55	1	37
2b	40	3.0	1.55	5	38
3	40	5.5	2.8	5	Not successful
4	60	3.0	1.55	0.037	37

¹ The strain rate representative for the field is unknown. The thermal induced contribution is expected to be fast and occurs mainly during start-up. The swell induced contribution is slower. Both contributions do not occur simultaneously. Since no effect of strain rate was found, 5 mm/min was selected based on practical experimental considerations.

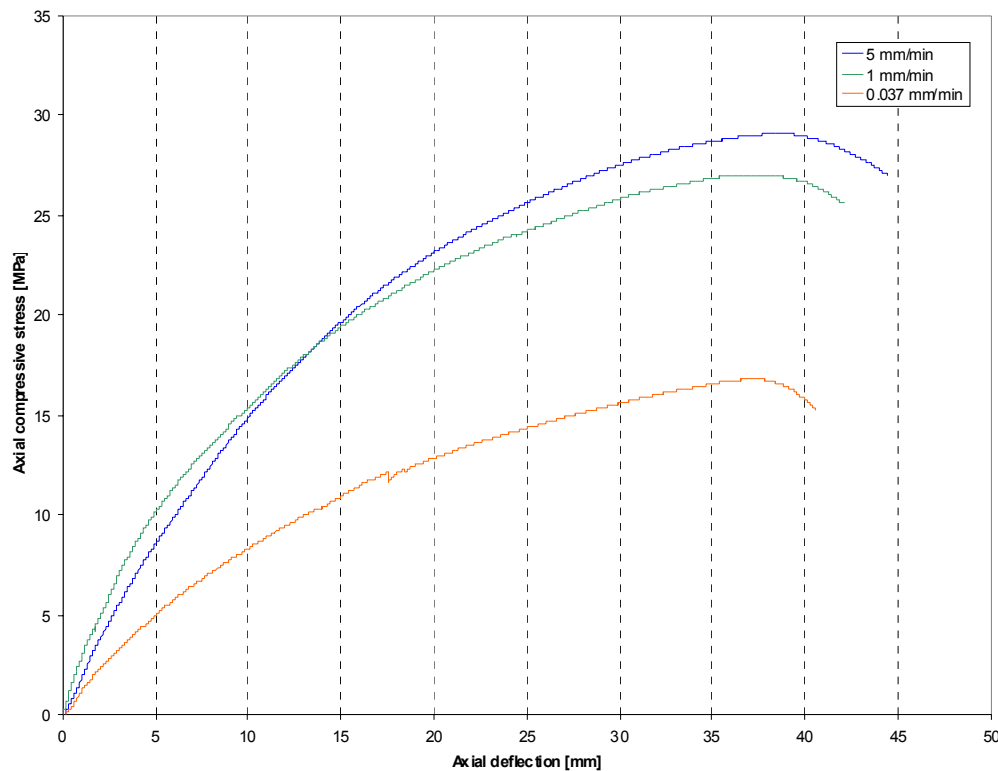


Figure 7

Axial compressive stress of HDPE as function of liner deflection at three different strain rates 0.037 mm/min at 60 °C, 1 and 5 mm/min (at 40 °C)

3.1.4.3 Determination imperfection size dependency

HDPE liner specimens with a SDR of 19.5 were tested at three different imperfection sizes, to determine the imperfection size dependency. An additional test was performed with an imperfection that covered only part of the circumference. For this test, only a part of the pins were used to create the imperfection. In total six of the 24 pins were used to make the imperfection of 1.5 mm. Table 5 shows the test parameters and critical deflections of HDPE liners. A plot of the results is shown in Figure 8.

Table 5 *Test parameters and critical deflections of HDPE liners*

Dimensions OD: 193 mm, t: 9.9 mm, L:320 mm

Test number	Temperature [°C]	Δ [mm]	IOD [%]	Strain rate [mm/min]	Critical deflection [mm]
5	80	1.9	1.0	5	38
6	80	4.5	2.3	5	32
7	80	1.5	0.8	5	47
8	80	3.0 (25 % pins)	1.6	5	37

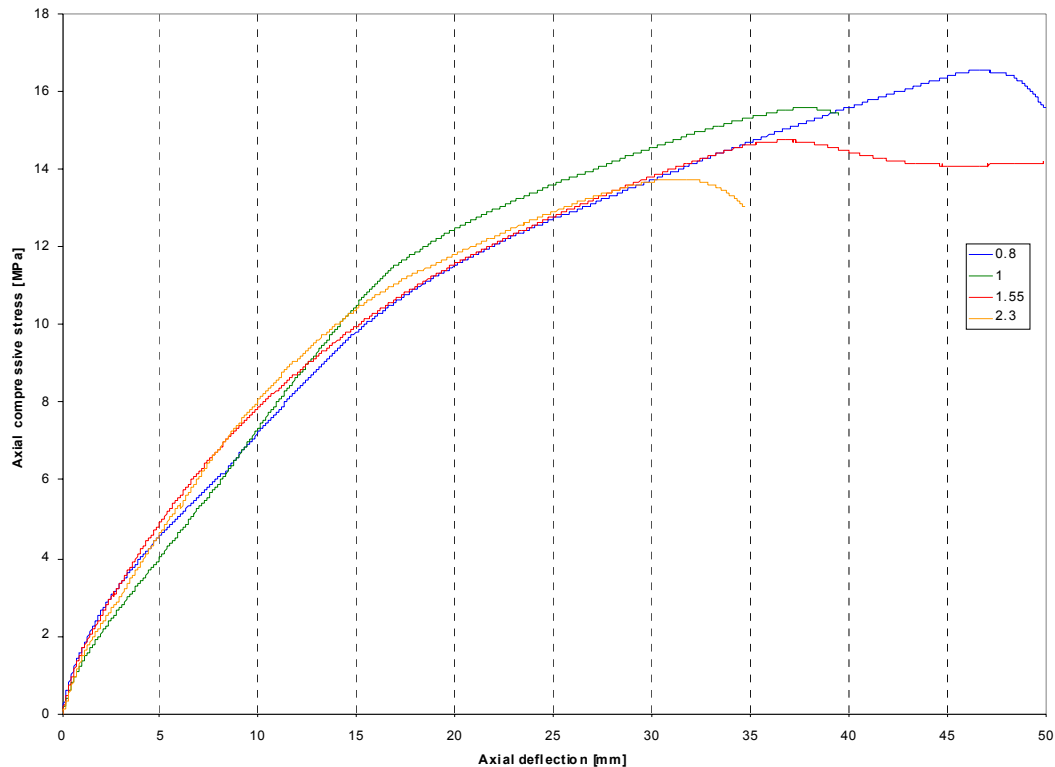


Figure 8

Axial compressive stress of HDPE as function of axial liner deflection for four different IOD imperfection sizes tested at 80 °C

3.1.4.4 Determination SDR dependency

PA-12 liner specimens with a SDR of 15 were tested at three different imperfection sizes, similar to the HDPE SDR 19.5 specimens to determine the imperfection size dependency and SDR dependency. Table 6 shows the test parameters and critical deflections of PA-12 liners. The tests were all performed at 20 °C assuming, based on the earlier tests at different temperatures, that temperature will not have an effect. A plot of the results is shown in Figure 9.

Table 6 *Test parameters and critical deflections of Evonik PA-12 liners (SDR 15)*

Test number	Temperature [°C]	Δ [mm]	IOD [%]	Strain rate [mm/min]	Critical deflection [mm]
1 + 2	20	1.5	2	5	Not successful
4	20	2.25	3	5	22
3	20	1.50	2	5	25
6	20	0.75	1	5	29
5	20	1.50	2	0.5	27

The interpretation and analysis of the obtained experimental results were done in combination with finite element analyses as discussed in the following sections.

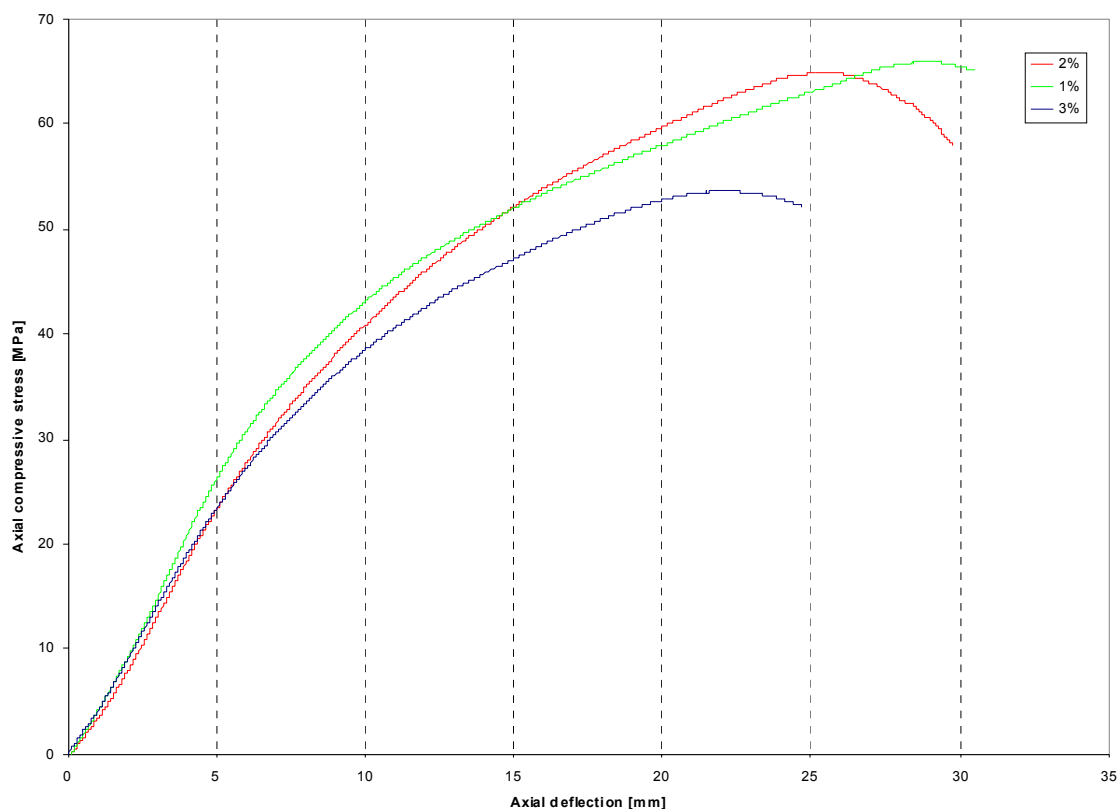


Figure 9

Axial compressive stress as function of axial liner deflection for Evonik PA-12 liners (SDR 15) for IOD values of 1,2 and 3 %, tested at 20 °C

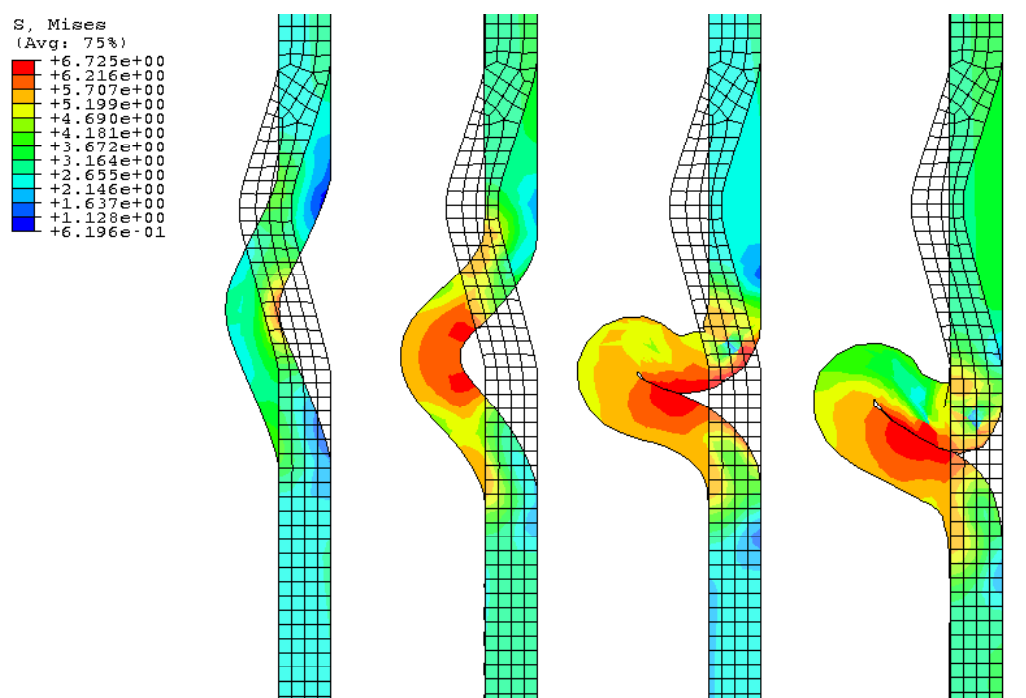


Figure 10

Finite element analysis simulation of the development of the buckling of a lobe. Buckling becomes unstable between the first and second drawing

3.1.5 Axial buckling and collapse modelling using finite element analysis

Finite element analyses were performed, as part of this study, to enhance the interpretation and analysis of the experimental results. Finite element analysis has been used before in two technical studies to model axial buckling and collapse of thermoplastic liners at elevated temperatures. Figure 10 shows a finite element analysis simulation of the development of the buckling of a lobe in a liner. The axial displacement is directed downwards.

To enhance the interpretation and analysis of the experimental results, test numbers 3 and 5 on the PA-12 liners tested at 20 °C were simulated using FEA. Two other FE analyses were performed to obtain the critical strain of test numbers 3, 5 and 6 on the PA-12 liners, however, for liners with a smaller wall thickness. Details about the FEA performed are provided in Appendix A.

Figure 11 shows of the axial force as a function of the axial displacement for the FE-model from liner tests 3 and 5 (ref. Table 5). The critical axial displacement determined using FEA was 23 mm. The experimental results were 25 mm for test 3 and 27 mm for test 5.

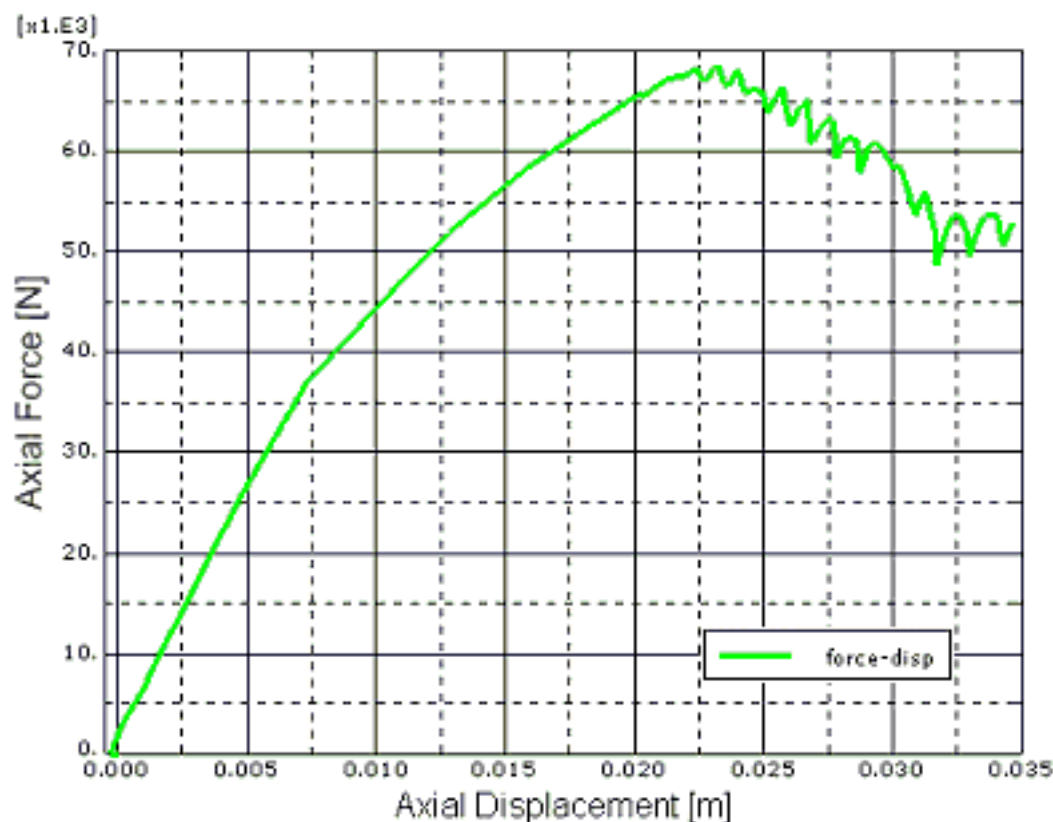


Figure 11

Axial force as function of the axial displacement for the FE-model from liner tests 3 and 5 (Evonik PA-12 material), from FEA

The difference between the FEA results and the test results for the experiments at 20 °C is between 14 and 23 %. This was considered accurate enough to simulate the axial buckling and collapse phenomenon. One or more of the following reasons were considered to cause differences between the FEA and test results:

- Differences found might be within the scatter of the test results, but the actual range of the scatter is unknown due to the small number of tests performed.
- The friction coefficient of 0.3 used in the FEA could be different from the friction coefficient in the tests, which was not determined.
- The actual material properties may not have been modelled accurately enough in the FEA.

3.1.5.1 Critical strain calculations

The output of the FEA was used to determine the critical strains.

The axial strain immediately below a lobe at the moment of collapse was taken as the value for the critical strain. In Table 7, the critical strains determined in the three different FEA are given.

Table 7 Critical strains for the performed FEA for Evonik PA-12 at 20 °C

FEA	SDR	IOD [%]	ϵ_{crit} [-]
1	15	2	0.09
2	18.75	2	0.07
3	18.75	1	0.10

The critical axial deflections determined in the axial buckling and collapse experiments required corrections before they could be used to determine the critical strain. FEA was used to determine the required corrections for the following effects²:

- Friction between liner and steel wall.
- Axial deflection due to deformation of the lobe.
- Support of the liner on the pins.

3.1.5.2 Correction for friction

The effect of the friction on the critical deflection was determined by performing FEA for two different friction coefficients. A friction coefficient of 0.30 resulted in a critical axial deflection of 23 mm and a friction coefficient of 0.05 resulted in critical deflection of 21 mm. Assuming a linear relation between the friction coefficient and the critical deflection gives, for zero friction, a critical deflection of 20.5 mm.

The Liner DEP indicates in Section 3.5.1 the following friction factors:

3.5.1 Friction load, $F_{friction}$

The friction load contribution to the overall liner pull-in load is derived from two components. One component is due to the weight of the liner and the associated friction factor, the other is due to superficial damage to the outside of the thermoplastic liner, i.e.:

where L_{liner} is the length of liner (m) to be installed and W is the weight of the liner per unit length (N/m). f is the friction factor and for new pipelines is taken as 0.4.

For retrofitting, higher friction factors may be required to simulate the surface roughness of the pipe. If the installation procedure includes liner lubrication then f should be reduced to 0.1. F_{score} is generally zero, unless otherwise quoted by the installer.

The friction coefficient of PA-12 on steel³ is between 0.3–0.4 very similar to the factor provided in the DEP. The critical axial deflections of the PA liners, therefore, were reduced by 2.5 mm to eliminate the effect of friction.

This correction is indicated by $d_{correction-friction}$.

² Note that the values of the obtained correction factors are estimates. It is not possible to determine accurate factors for all tests using FEA results based on one model.

³ <http://www.matbase.com/material/polymers/engineering/pa-12/properties>.

3.1.5.3 Correction for lobe deformation

The axial deflection measured in the tests is the sum of the axial compressive strain times the length of the liner and at the point of collapse the, localised, axial deformation of the lobe. Since the length of the liner specimens was relatively short, the contribution of the lobe deformation on the axial deflection cannot be ignored and has to be compensated for in order to determine the critical strain. In order to calculate the average critical strain from the measured total displacement in the mechanical test, the displacement was corrected for the deformation of the lobe. This correction factor was derived by performing FEA simulating the mechanical test. The correction factor was determined calculating the difference in axial distance between two nodes at the boundary of the lobe at the unloaded condition and at the critical deflection. The maximum in the load-displacement curve was used as the critical deflection.

The correction was performed as follows:

- Critical deflection. The node at the lobe with the largest radial inward displacement was selected (red dot in Figure 12(b)). This node was used as the reference point to define the distance between the two yellow nodes, defining the boundaries of the lobe. The distance between the yellow nodes is indicated as d_{after} .
- The original distance between these two yellow nodes in the unloaded condition was determined (d_{before}), using the red node as the reference node (left drawing in Figure 12(b)).
- If no lobe would form (i.e. no imperfection), the deformation of the section between the two yellow nodes (i.e. the 'lobe section') at the strain level equal to the strain at the onset of axial collapse is defined as:

$$d'_{before} = d_{before} * (1 - \varepsilon) \quad (7)$$

Where:

d'_{before} = the distance between the two yellow nodes at the strain level equal to the strain level at the critical deflection.

d_{before} = the distance of the two yellow nodes in unloaded condition.

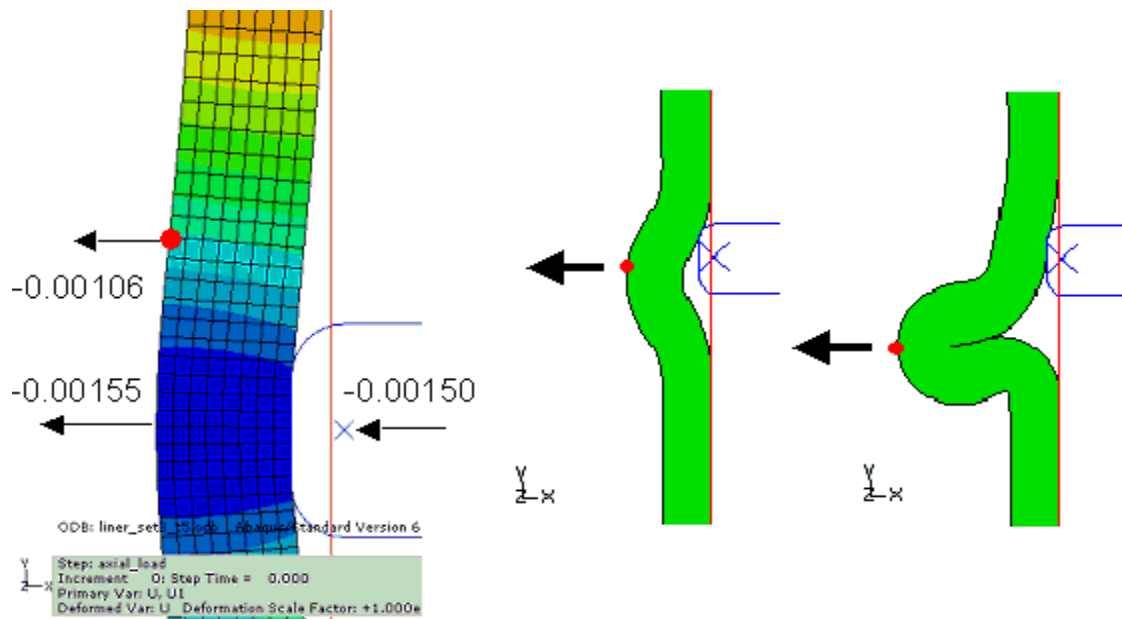
ε = the strain at critical deflection. This strain is taken from a node located just below the lobe.

The actual displacement can be calculated from the measured displacement as follows:

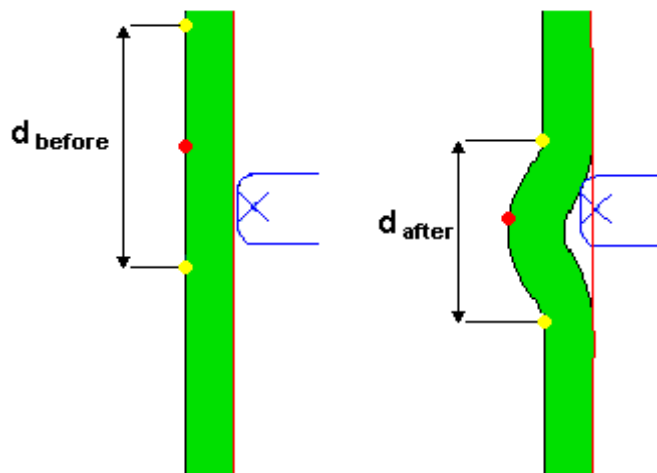
$$d_{correction-lobe} = d_{measured} - \Delta d \quad (8)$$

Where:

$$\Delta d = d'_{before} - d_{after} = d_{before} * (1 - \varepsilon) - d_{after} \quad (9)$$



(a)



(b)

Figure 12

Red, node with maximal radial displacement at moment of collapse.

Yellow nodes, used for the displacement correction for lobe deformation

In Figure 14 the radial inward displacement of a lobe is shown for two different SDR values. The displacement at the critical deflection is similar, therefore, no correction factor is applied to compensate for the difference in SDR.

The FEA simulating a smaller imperfection shows that the radial inward displacement is dependent on the size of the imperfection, but most of the difference is caused by the difference in initial radial displacement. It is, therefore, not necessary to use different correction factors for liners with different imperfection sizes.

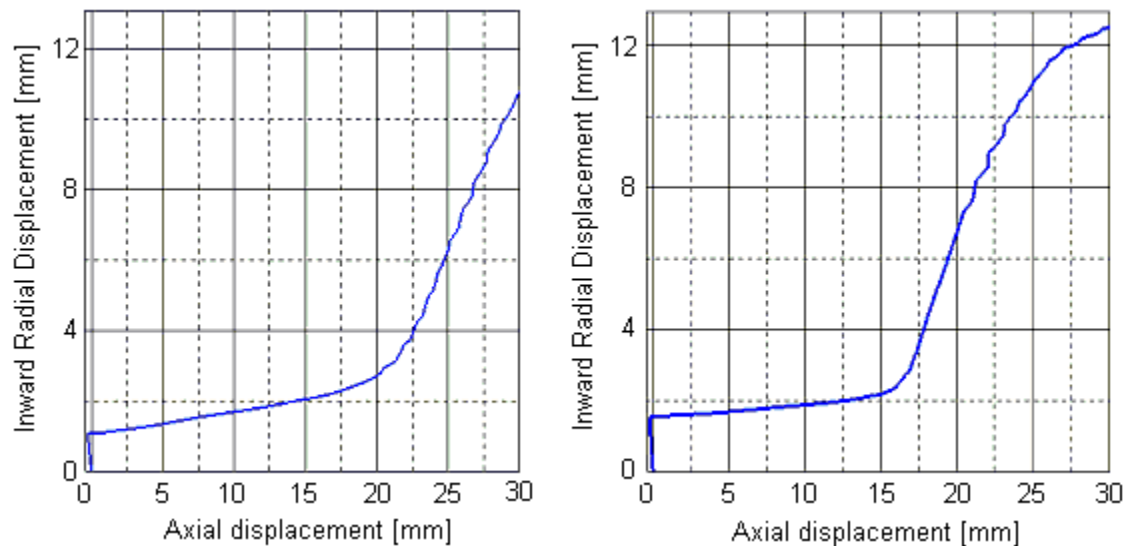


Figure 13 Inward radial displacement of liner with SDR 18.75 (left) and SDR 15 (right)

3.1.5.4 Correction for pin support

Score marks found on the liner specimens indicated that the pins used to create the radial imperfections were supporting the liner during the tests. Estimating the influence of the pin support on the critical axial deflection proved difficult, since precise modelling of the pins was complex. The friction coefficient between the pins and the liner is zero, the strain directly before and after the lobe should be similar when the pins are not supporting the liner. The results of the model show that the difference in strain before and after the lobe is 5 % for an imperfection of 1.5 mm and 4 % for an imperfection of 0.75 mm. The displacement correction factors ($d_{\text{correction-pin}}$) for these additions to the lobe (length is 70 mm) are 3.5 mm and 2.8 mm.

The difference between the FEA and the actual tests is that the imperfection in the model is a continuous circumferential pin and the pins in the test have a diameter of 8 mm with 12 mm spacing in between the pins. The liner support of the pins in the tests is, thus, less than in the FEA. For the imperfection of 1.5 mm, a correction factor of 1.75 was used for and, for the imperfection of 0.75 mm, a correction factor of 1 mm was used.

3.1.5.5 Overall displacement correction

The critical strain was calculated from the displacement measured in the mechanical axial collapse experiment using the following equation:

$$\varepsilon_{\text{critical}} = \frac{d_{\text{measured}} - d_{\text{correction-friction}} - d_{\text{correction-lobe}} - d_{\text{correction-pin}}}{L_{\text{liner-specimen}}} \quad (10)$$

In Table 8, correction factors are listed for the tests that were used to determine the critical strain. The correction factors from the HDPE liners are determined by scaling the factors from the PA-12 in accordance with the difference in dimensions of both sets.

Table 8

Value of the correction factors and the resulting critical strain for HDPE (SDR 19.5) liners and PA-12 liners

Set	Test number	Critical axial deflection [mm]	Factor friction [mm]	Factor lobe [mm]	Factor pin-support [mm]	ϵ_{crit} [-]
PA-12	3	25	2.5	4	1.75	0.093
PA-12	4	22	2	4	2.5	0.073
PA-12	6	29	3	4	1	0.117
HDPE (SDR 19.5)	2a	37	4	6	1.5	0.080
HDPE (SDR 19.5)	2b	38.5	4	6	1.5	0.084
HDPE (SDR 19.5)	4	37	4	6	1.5	0.080
HDPE (SDR 19.5)	5	38	4	6	1.25	0.084
HDPE (SDR 19.5)	6	31.5	3	6	2	0.064
HDPE (SDR 19.5)	7	47	5	6	1	0.109

3.2 Axial collapse equation

The Buckingham Pi Theorem [5] was used to perform a dimensional analysis of the axial collapse. The Buckingham Pi Theorem is a statement of the relation between a function expressed in terms of dimensional parameters and a related function expressed in terms of non-dimensional parameters.

All parameters involved were determined. These are the critical axial collapse stress σ_{crit} , the elastic modulus $E(T)$, the diameter D , the wall thickness t , the friction and the dimensions of the imperfection Δ and L . Assuming no friction and imperfections. This will result in the following function:

$$\sigma_{crit} = f(E, D, t) \quad (11)$$

The Buckingham Pi Theorem was used to find out whether this function could be written in terms of fewer parameters.

Equation (11) can be written as:

$$\sigma_{crit} = ZE^a t^b D^c \quad (12)$$

in which Z , a , b and c are dimensionless constants. The dimensions of the left hand side of Equation (12) have to be the same as the dimensions on the right hand side. This is used to reduce the number of constants. Defining the dimensions as follows:

- F is a force.
- L is a length.

Equation (12) can be written in terms of the dimensions and equations for the constants can be determined for each separate dimension:

$$FL^{-2} = (FL^{-2})^a (L)^b (L)^c \quad (13)$$

Consider F : $1 = a$

Consider L : $-2 = -2a + b + c$

Solving for a , b and c leads to

$$a = 1$$

$$b = -c$$

Finally, Equation (12) can be written as follows:

$$\sigma_{crit} = cE \left(\frac{t}{D} \right)^n \quad (14)$$

where:

- σ_{crit} = critical stress at moment of collapse
- E = Young's modulus
- c = coefficient function of liner undersize and/or imperfection
- n = power n is a function of liner undersize and/or imperfection
- D = the outer diameter (mm)
- t = the wall thickness in (mm)

With $\sigma_{crit} = \epsilon_{crit} E$ this can be rewritten as:

$$\epsilon_{crit} = c \cdot \left(\frac{1}{SDR} \right)^n \quad (15)$$

- ϵ_{crit} = critical axial deformation, point of collapse
- c = coefficient function of liner undersize and/or imperfection
- n = power n is a function of liner undersize and/or imperfection
- SDR = Standard Dimension Ratio D/t

In this equation, it is assumed that the axial collapse process is elastic (Hooke's law). In reality, a polymer shows an elastic-plastic behaviour. For the materials investigated here (HDPE and PA-11), the stress-strain curve is affected by temperature but the strength/stiffness ratio remains roughly the same. Whether this behaviour is true for other polymers or polymer grades is unknown.

For the strain-rate dependency, a similar behaviour is observed. Also here, the stress-strain curve is affected significantly by the strain rate but the strength/stiffness ratio remains roughly the same.

The equation for axial collapse is similar to the equation for radial collapse. The difference is the values of the two constants in the equations. Dimensional analysis was used to determine the influence of the size of the imperfection on the critical stress. The variables for the dimensions of the imperfection are defined in Figure 14. The diameter is also a variable.

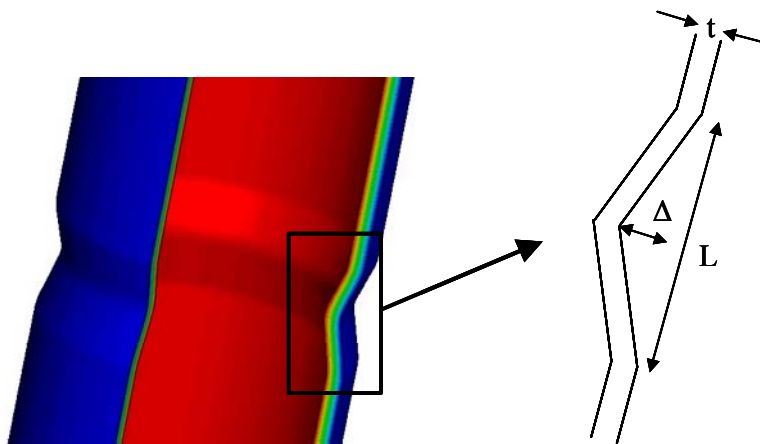


Figure 14 Variables for the dimensions of the imperfection

All four variables have length as a dimension. A further reduction of the number of variables in the collapse equation using dimensional analysis is, therefore, not possible.

From this equation, it follows that the axial collapse is deformation (strain) driven, and independent of the stiffness of the material. The exponent n is a function of the size of the Imperfection On Diameter (IOD).

Similar as for the radial collapse coefficient, c was kept constant and 1 and the factor n was determined on the basis of experiments and finite element analysis.

The constant Z and factor b in Equation (12) were determined using the critical strains listed in Table 7. Two equations with two unknowns are obtained for a specific value of the IOD when two critical strains, one from liner set 2 and one from set 3, are taken from tests performed with the same IOD. Solving the equations for the range of tested IOD values results in functions of Z and b as a function of the IOD.

The values of Z and b are rapidly increasing with an increasing value of the IOD. Small fluctuations of the critical strain result in large variations of the determined values of Z and b . The critical strains used for the derivation have an uncertainty up to 10 % due to the variation in test results and they thus cause large deviations in the determined values of Z and b . Therefore, it is not possible to determine an accurate best-fit equation of the values of Z and b as, function of the IOD through the calculated data points.

Instead of using values of Z and b that are both dependent on the IOD, only factor b was taken as a variable. This made it possible to determine the factor b for each individual test and FEA result. A best-fit equation of the factor b as a function of the IOD was determined through the calculated values of b . The value of Z was set on 1 and the value of the factor b is calculated for each test with the equation below.

$$b = \frac{\log\left(\frac{\varepsilon_{crit}}{Z}\right)}{\log\left(\frac{1}{SDR}\right)} \xrightarrow{Z=1} b = \frac{\log(\varepsilon_{crit})}{\log\left(\frac{1}{SDR}\right)} \quad (16)$$

In Figure 15 is a linear and logarithmic best-fit (least squares) equation plotted through the data points. The R^2 values of both equations show that the logarithmic equation has a larger reliability than the linear equation, but the difference is small. The range of investigated IOD is not large enough to prove which one of the equations is right. It is decided to use the linear equation, because this equation is the most conservative outside the range of investigated IOD.

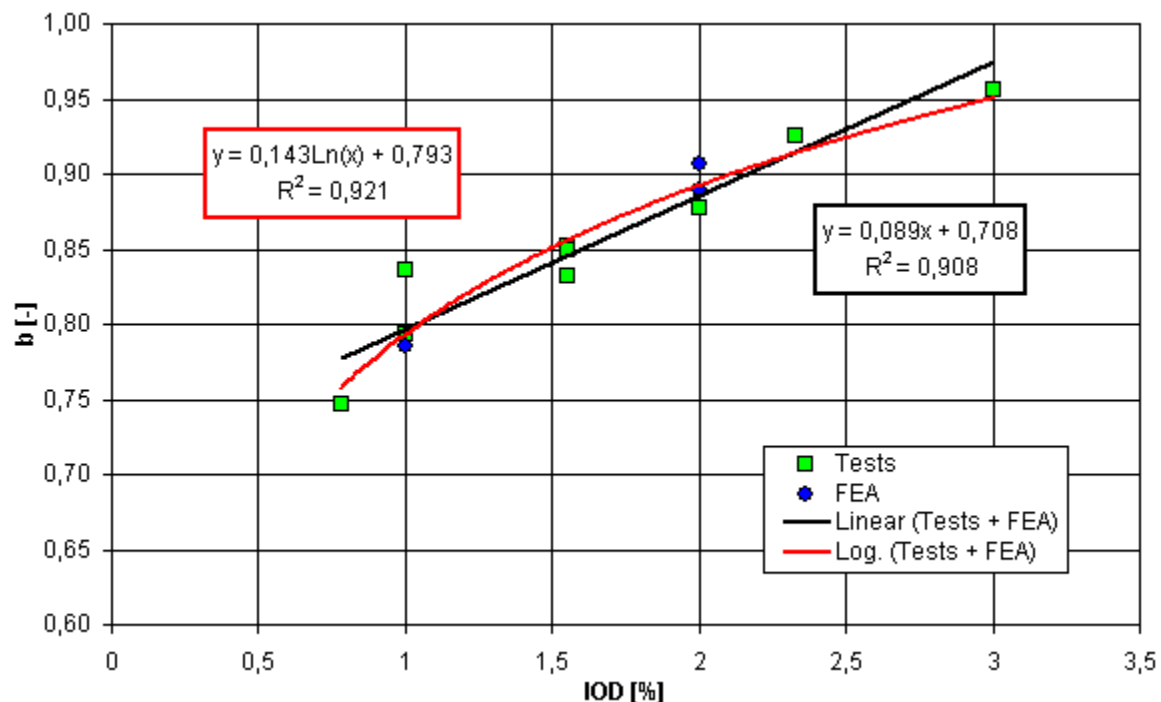


Figure 15 Linear and logarithmic best-fit equations for factor b through test and FEA data

3.3 Acceptance criterion for axial strain

The critical axial strain can be calculated with the following engineering equation:

$$\varepsilon_{crit} = \left\{ \frac{1}{SDR} \right\}^n \quad (17)$$

with :

$$SDR = \frac{OD}{t}$$

$$b = 0.089.IOD + 0.708$$

An alternative approach to derive axial collapse equation based on maximum push load calculation method is provided in Appendix B.

The strain that is calculated with Equation (17) is the critical strain in axial direction that will cause an instable axial buckling of the liner. As long as the induced axial strain in the field application is smaller than this critical strain, the liner is resistant against axial collapse:

$$\varepsilon_{crit} \leq \varepsilon_{ax} \quad (18)$$

Introducing a safety factor, Equation (18) can be written as:

$$\varepsilon_{crit} \leq \varepsilon_{ax} \cdot SF \quad (19)$$

3.3.1 Axial strain in liner during service

The total axial strain induced in a field application is equal to the sum of:

- (a) The thermal induced strain.
- (b) The linear swell induced strain.
- (c) The hoop strain induced axial strain.

$$\varepsilon_{ax} = \varepsilon_{lin} + \varepsilon_{thermal} + \nu(\varepsilon_{lin} + \varepsilon_{thermal}) \quad (20)$$

The thermal induced strain is equal to:

$$\varepsilon_{thermal} = \alpha \cdot \Delta T \quad (21)$$

in which:

$$\Delta T = T_{design} - T_{instal}$$

The axial strain due to swell can be derived from the volumetric swell and can be written as:

$$\varepsilon_{lin} = \sqrt[3]{(1 + \Delta V) - 1} \quad (22)$$

Substitution of Equations (21) and (22) into (20) gives:

$$\varepsilon_{ax} = (1 + \nu) \left\{ \sqrt[3]{\Delta V + 1} - 1 + \alpha \cdot \Delta T \right\} \quad (23)$$

With:

ΔV the volumetric swell (fraction)

ε_{ax} the axial strain (fraction)

Appendix C provides full details.

The acceptance criterion (18) can be rewritten as:

$$\varepsilon_{crit,ax} > \varepsilon_{ax} \quad (24)$$

Equations (17) + (25) gives:

$$\left\{ \frac{1}{SDR} \right\}^n > \varepsilon_{ax} \quad (25)$$

Equation (25) can be rewritten to define the required minimum wall thickness or the required maximum SDR to avoid axial liner collapse:

$$t > OD \cdot \sqrt[n]{\varepsilon_{ax}} \quad (26)$$

and:

$$SDR < \left\{ \sqrt[n]{\varepsilon_{ax}} \right\}^{-1} \quad (27)$$

3.3.2 Field factors

In the next paragraphs, the influences of friction, pre-tensioning on the axial collapse equation are described. It is also investigated which size of the imperfection has to be used during the design of the liner. After that, the equation is used to analyze a failure that occurred in the field. Finally, it is described which changes have to be made in the flange design to allow disconnection of the flanges for maintenance after a service period.

3.3.2.1 Friction

In an actual field application, friction between the liner and the host pipe is not expected to have an influence on the collapse of the liner. The axial strain is built up by the thermal expansion and swell.

The stress and strain might be somewhat lower at the ends of the lobe than further away from the lobe at the moment that the lobe has a large radial inward displacement, since the liner is sliding over the host pipe to increase the size of the lobe. The radial inward displacement, however, is still small at the moment of collapse and the liner will not have shown noticeable sliding in the host pipe. Friction is, therefore considered to be negligible.

3.3.2.2 Pre-tensioning

After installation, the liner is normally pulled a few meters out of the host pipe on both sides of the section, the purpose is to introduce an axial strain. The DEP indicates a practical allowance of 20 mm per 10 m of pipe for each 10 °C change in temperature.

The ends are cut off and the flanges are welded on the end of the liner. When the liner is released, the induced axial stress will pull the liner inside the host pipe till the flanges of the liner are positioned on the flanges of the host pipe.

Part of the axial stress will remain after releasing the liner. Pre-tensioning has a positive effect on the total axial strain after saturation, because the tensional strain after installation can be subtracted from the total axial strain caused by the thermal expansion, swell and bending induced compressive strain. In the design procedure, the positive effect of pre-tensioning on the axial collapse resistance of the liner was not taken into account since, in actual field applications, it is difficult to quantify. This means that the proposed design criterion is conservative.

3.3.3 Imperfection size

Weld protrusions in the steel host pipe are typical imperfections expected to be found in the field. The height of the root cap with respect to the wall of the steel pipe is dependent on the welding technique. Pipeline engineers expect weld protrusions of a maximum size of 5 mm.

The Liner DEP indicates in Section 5.4.2.5 the following related requirement.

From 5.4.2.5 Wireline and pig train

The liner test segment attached to the pig train should emerge without serious damage. Scuffing of the liner surface is permissible but sharp longitudinal scars or other penetration damage exceeding 0.5 mm or 5 % of the wall thickness, whichever is larger, is unacceptable and would require rectification by further pigging using a breaker pig or by other means before continuing with liner installation. After rectification another liner test segment should be pulled through.

Based on this DEP section, a 5 mm imperfection would be equal to 5 % of a 100 mm thick liner, which is a very thick liner hardly even user. A maximum imperfection size of 5 mm is, therefore, currently considered as conservative.

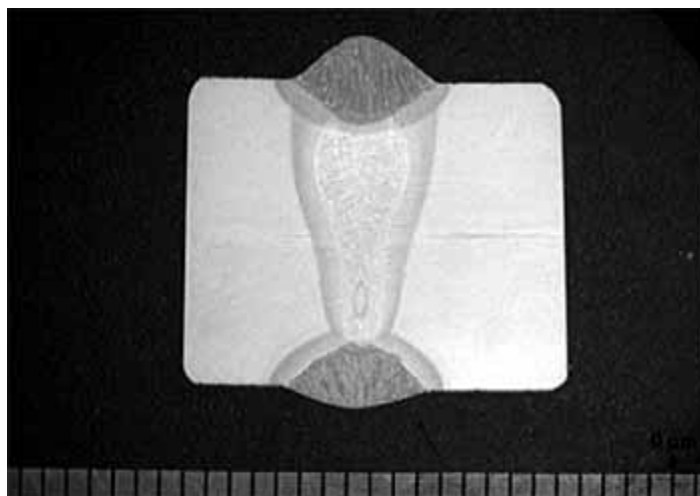


Figure 16 Typical root cap of a welded steel pipe

During operation, a large pressure is applied in the bore of the liner. For liners with a wall thickness that is several times larger than the imperfection, this pressure will probably press the imperfection into the liner wall without causing an imperfection at the inner side of the liner. This would lead to a critical strain that is smaller than calculated with Equation (17).

3.3.4 Flanges

Maintenance and/or repair efforts during the service life of the liner, might require the flanges of a liner section to be disconnected. Field observations indicate that after disconnection of the flanges, the liner often moves up substantially out of the host pipe. This is most likely the result of an elastic compressive strain in axial direction caused by the thermal expansion and swelling. Outside the host pipe, the liner diameter can expand due to elastic strains in hoop direction. As such, it often not possible to push the liner back into the host pipe.

A representative from a liner contractor⁴ once indicated that this, potentially, was one of the main reasons to limit the operating temperature of polymer liners.

3.3.5 Field experience axial failure

The liner properties and operating conditions of a liner that failed due to axial collapse were used as input for the axial collapse design equation. The objective was to determine whether the failure could be explained based on this method. The properties of the liner are listed in Table 9.

⁴ Verbal communication with a representative from United Pipeline Services.

Table 9 *Characteristics of failed liner*

Liner material	HDPE
Service	Produced water
Installation temperature	20°C
Operating temperature	93°C
Diameter	16 inch
Wall thickness	10 mm
SDR	40.6
Length	21 km
Number of failed sections	2
Imperfection (assumed)	5 mm
Bends in certain sections	yes
Poisson's ratio	0.4

$$IOD = \frac{5}{16 \times 25.4} \times 100\% = 1.2\%$$

$$b = 0.089 \times 1.2 + 0.708 = 0.817$$

$$\varepsilon_{crit} = \left(\frac{1}{40.6} \right)^{0.817} = 4.8\%$$

The axial strain due to thermal expansion of the liner is:

$$\varepsilon_{thermal} = (1 + \nu)\alpha\Delta T$$

If bending is assumed to be fully corrected by pre-tensioning and swell is assumed to be zero, the total induced axial strain due to thermal expansion is:

$$\varepsilon_{thermal} = (1 + 0.4) \cdot 200 \cdot 10^{-6} \cdot (93 - 20)$$

The calculation gives a critical strain of 4.8 %. The total axial strain is smaller than the critical strain

The liner failed due to radial collapse in two of its 36 sections. Axial collapse could have occurred when an additional 2.8 % axial strain was present. e.g. due to swell or bending in combination with insufficient applied pre-load. Some sources⁵ have reported that the allowable minimum-bending radius is a function of the SDR of the liner. The larger the SDR, i.e. the lower the wall thickness, the larger the minimum allowable bending radius. This might have also played a role in the explanation of this failure.

Due to the low wall thickness, the liner also had a radial collapse resistance of less than one bar, such that an axial collapse in case of vacuum cannot be excluded and seems to be more likely.

3.4 Required material properties for axial buckling calculations

For axial buckling design calculations for the application in hydrocarbon service, the following properties are required:

- Coefficient of Thermal Expansion (CTE) as function of temperature.
- Swell behaviour of the PA-12 polymer for the envisaged service.

⁵ Polyethylene Piping Systems Manual, Driscopipe <http://www.driscopipe.com>.

Service fluids of the oil and gas industry are typically multi component mixtures and accurate predictions and/or interpolation of extrapolations on the basis of a single fluid property is not always feasible. The API density of different crude oils showed to be an acceptable property.

For a more versatile use of the design equations for a range of hydrocarbon services, it is recommended to carry out swell experiments in at least 3 different API grades and at least three different temperatures.

3.5 Water service with low concentration of crude oil

The low solubility of crude oil in water results in a high activity even for very low concentrations, ppm level, of crude oil in water. Therefore, even thermoplastic liners envisaged for water service with very low concentration of crude oil should be designed similar as those in crude oil service.

Low gas to liquid ratios will result in a delay of pressure build up in the annulus but the final effect will remain similar to high gas to liquid ratio.

3.6 Polyamide PA-12 versus HDPE

From the axial buckling model, it follows that the buckling resistance only depends on the CTE and swell of the polymer material. In earlier investigations, it has been found that the swell of PA-12 in hydrocarbons is significantly, lower compared to that of HDPE (see Appendix D), which is beneficial in terms of buckling resistance. However, the total induced axial strain also depends on the coefficient of thermal expansion and this can vary between the different PA-12 and HDPE grades.

4. Discussion of results

A method for the determination of axial collapse has been developed and a good comparison with experimental results and FEA was obtained.

Assumptions included:

- In the design equations, the materials are assumed to follow a full elastic behaviour. In reality, the materials show an elastic-plastic behaviour. In the finite element analysis however, the full elastic-plastic stress-strain responses for HDPE and PA-11 have been used and showed an acceptable correlation with the lab experiments.
- For other polymer materials and/or material grades, the findings as described above have to be validated.

5. Conclusions

- (a) An axial buckling model has been developed and verified with experimental laboratory tests and FEA. The FEA results showed a good agreement with the of the laboratory tests results.
- (b) A simplified field applicable design equation has been provided for axial collapse.

6. Recommendations

For liners with a wall thickness that is several times larger than the imperfection, a high bore pressure will probably press the imperfection into the liner wall without causing an imperfection at the inner side of the liner. This would lead to a critical strain that is smaller than calculated with the derived design Equation (17). It is recommended to confirm this hypothesis including the influence of the ratio of the IOD and the wall thickness of the liner.

To enable a full liner design calculation for PA-12 material, the availability of the polymer volumetric swell as function of the temperature and API grade of the hydrocarbon fluid will be required. It is recommended to carry out exposure tests of the PA-12 polymer material to a range of API crudes and temperatures.

For a more versatile use of the design equations for a range of hydrocarbon services, it is recommended to carry out swell experiments in at least 3 different API grades and at least three different temperatures.

The low solubility of crude oil in water results in a high activity even for very low concentrations, ppm level, of crude oil in water. Therefore, even thermoplastic liners envisaged for water service with very low concentration of crude oil should be designed similar as those in crude oil service.

It is recommended to design special flanges for liners operating at elevated temperatures such that the liner is prevented from moving out of the host pipe when the flanges of the sections are disconnected. It is preferred to do this in a way such that the standardized steel flanges of the host pipe do not have to be changed. The design should take into account that liner flanges are preferably manufactured by moulding and/or milling.

In the design equations, the materials are assumed to follow a full elastic behaviour. In reality the materials show an elastic-plastic behaviour. In the finite element analysis however, the full elastic-plastic stress-strain responses for HDPE and PA-12 have been used and showed an acceptable correlation with the lab experiments. For other polymer materials and/or material grades, the findings as described above have to be validated.

7. References

- 1 Sklarz, K.E., 'Non-Metallic (Thermoplastic) Liners For Sour Gas Pipelines', EUROCORR 2007.
- 2 De Mul, L.M. , van de Haterd, N. Gerretsen J.H., 'Experiences With Polyethylene Lined Systems in Oman'. Authors L.M. de Mul, Shell International Oil Products; Nol van de Haterd, Shell International; J.H. Gerretsen, NACE CORROSION 2000, March 26 - 31, 2000 , Orlando, Paper Number 00788.
- 3 Szklarz, K.E., Baron, J. NACE Paper Number 04702 , 'Learnings from Thermoplastic Liner Failures in Sour Gas Pipeline Service and Replacement Liner Design and Installation' March 28 - April 1, 2004 , New Orleans.
- 4 Goerz, K., Simon, L. Fear, H., Little, J., A Review of Methods for Confirming Integrity of Thermoplastic Liners - Field Experiences CORROSION 2004, March 28 - April 1, 2004 , New Orleans. 04703.
- 5 Buckingham, E. (1914). 'On physically similar systems; illustrations of the use of dimensional equations'. Phys. Rev. 4: 345–376.

Amsterdam, December 2009

qts

Appendix A. Results F.E.A. Ruben van Schalkwijk

Lining CollapsePage 1



Shell GS Amsterdam


Axial Lining Collapse
version 3
Ruben van Schalkwijk, 24 March 2009




Copyright 2009 RvS-Engineering

Lining CollapsePage 2

Material Model PA-12



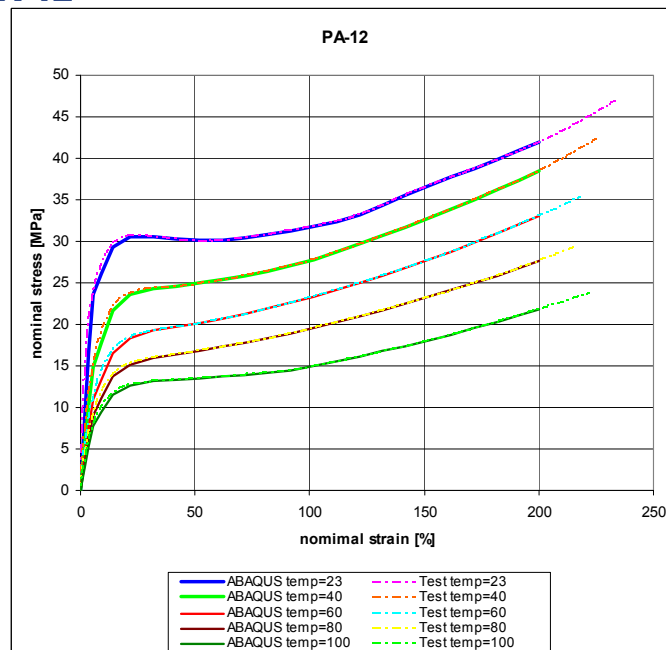
- Uni-axial PA-12 material tensile test data are available for a range of temperatures
- A temperature dependent elasto-plastic model is used
- The elasticity and the true-yield stress versus true plastic strain is determined from the nominal stress versus nominal total strain test results
- To verify the results a simple tensile ABAQUS model is made to reproduce the test by simulation. See next slide.

Copyright 2009 RvS-Engineering

Material Model PA-12

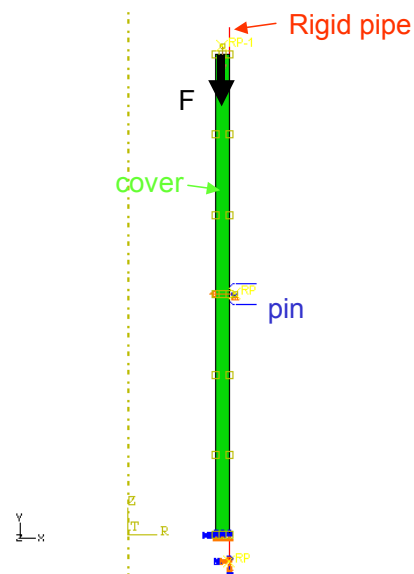
- Test-model

- ABAQUS model
- Experiment



Axial collapse model

- Axi-symmetrical cover model
- Rigid pipe
- Imperfection: rigid pin



Axial collapse model

- **Load history**

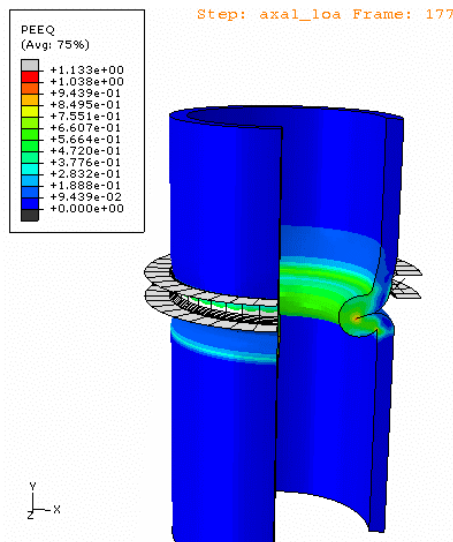
- Initial temperature 20 [°C]
- Imperfection: move the pin inwards
- Increase the temperature
- Apply the axial load

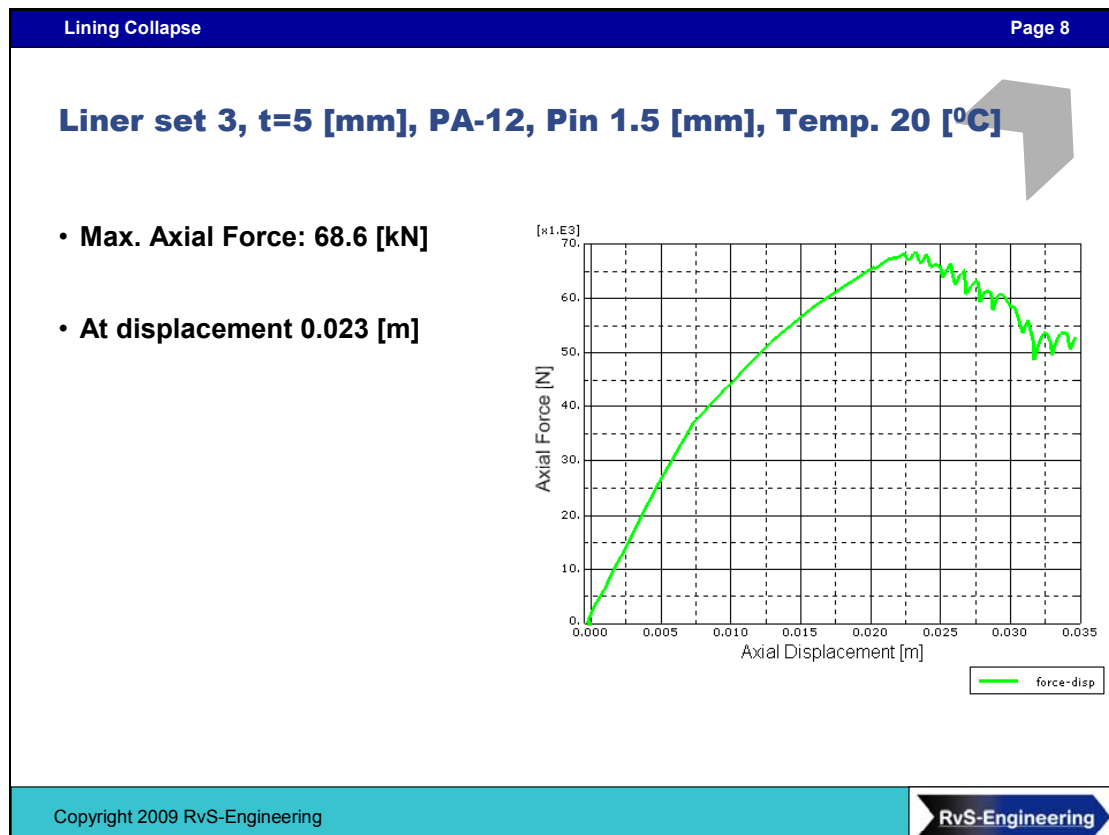
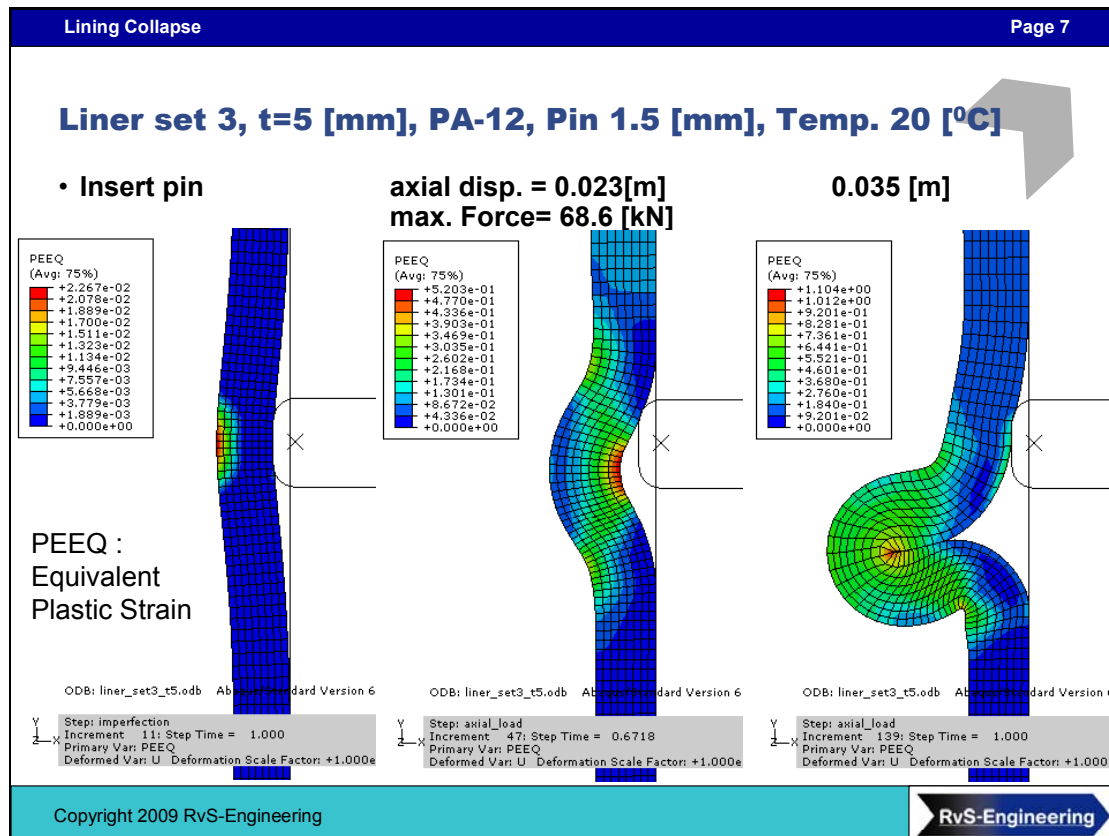
- **Contact interactions**

- Cover to rigid pipe, friction coefficient 0.3
- Cover pin, no friction
- Cover Self contact, no friction

Animation: example case

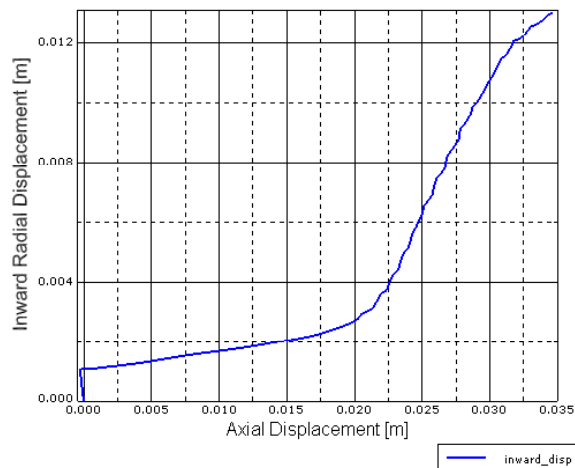
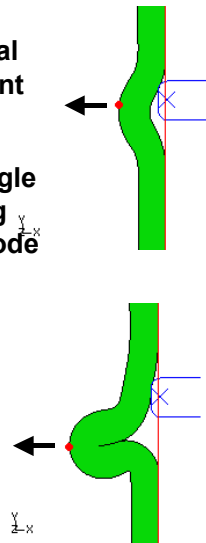
- **Animates in full screen Slide Show mode**





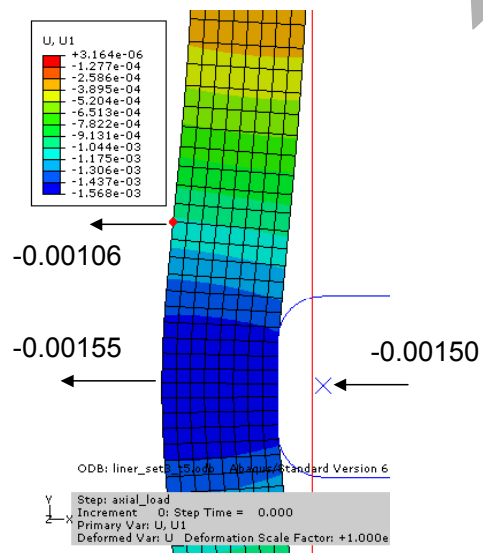
Liner set 3, $t=5$ [mm], PA-12, Pin 1.5 [mm], Temp. 20 [°C]

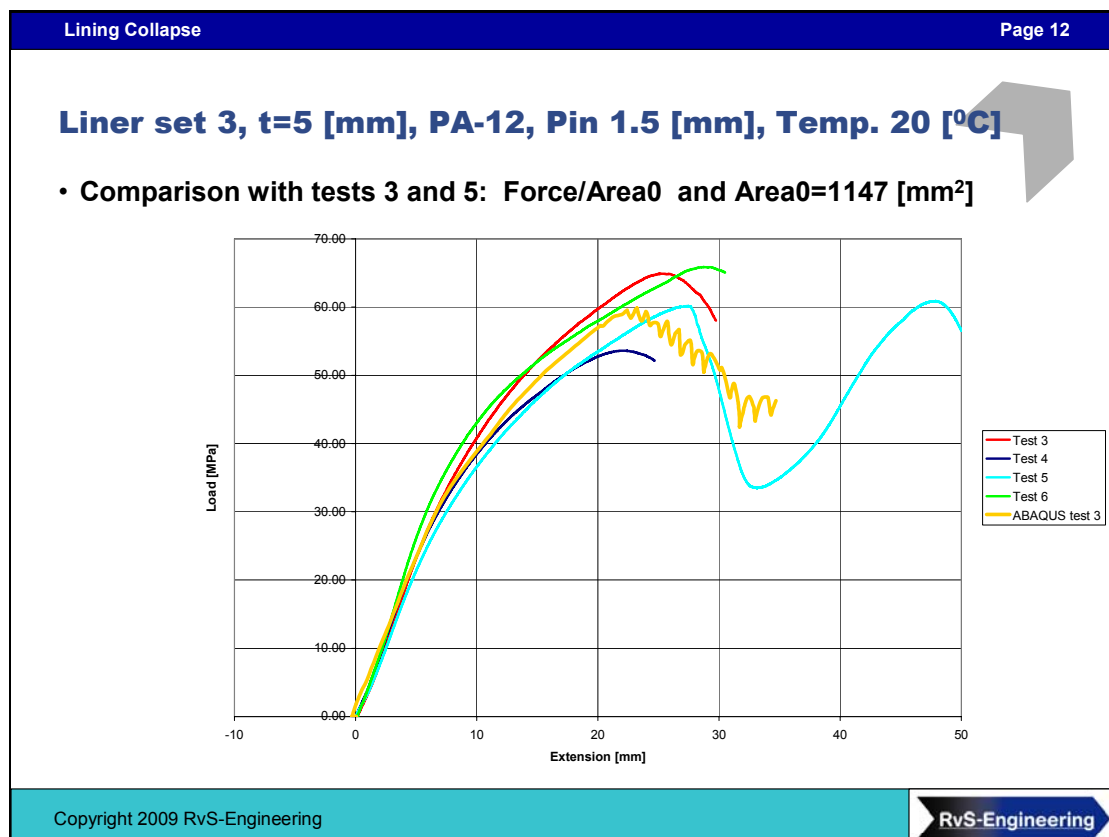
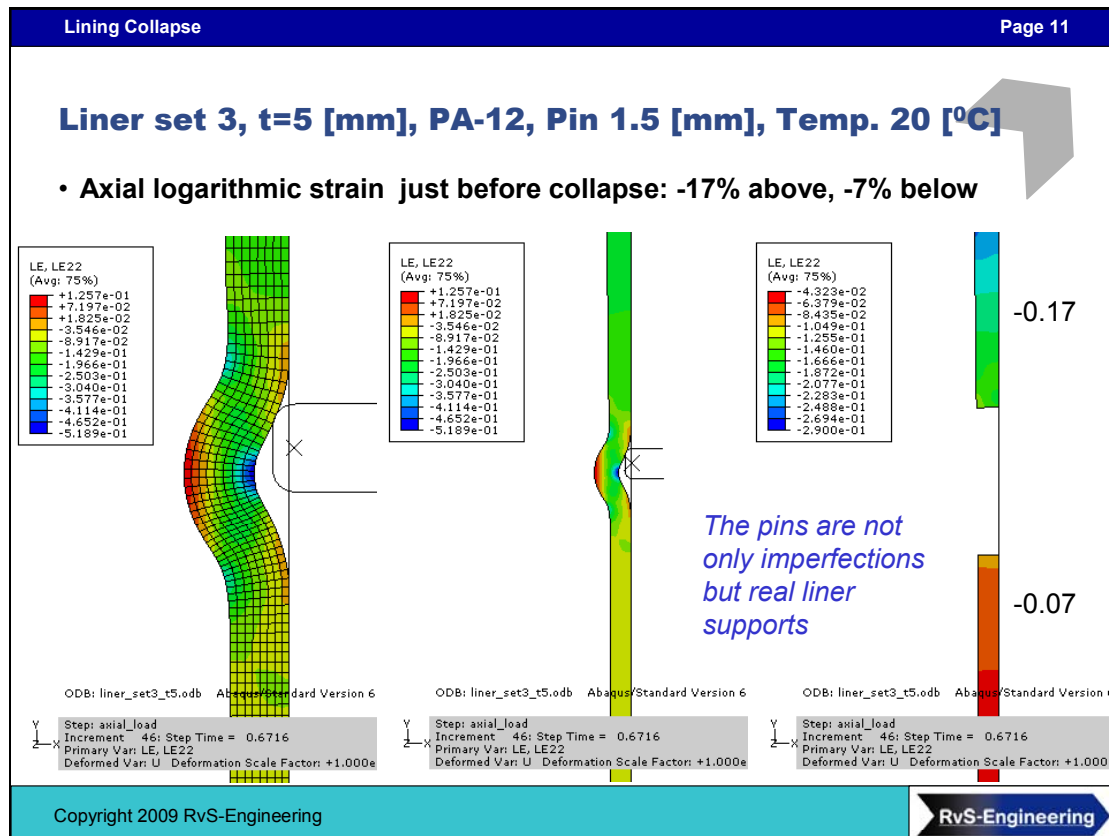
- Inward radial displacement
- Monitor single node during analysis (node 129)

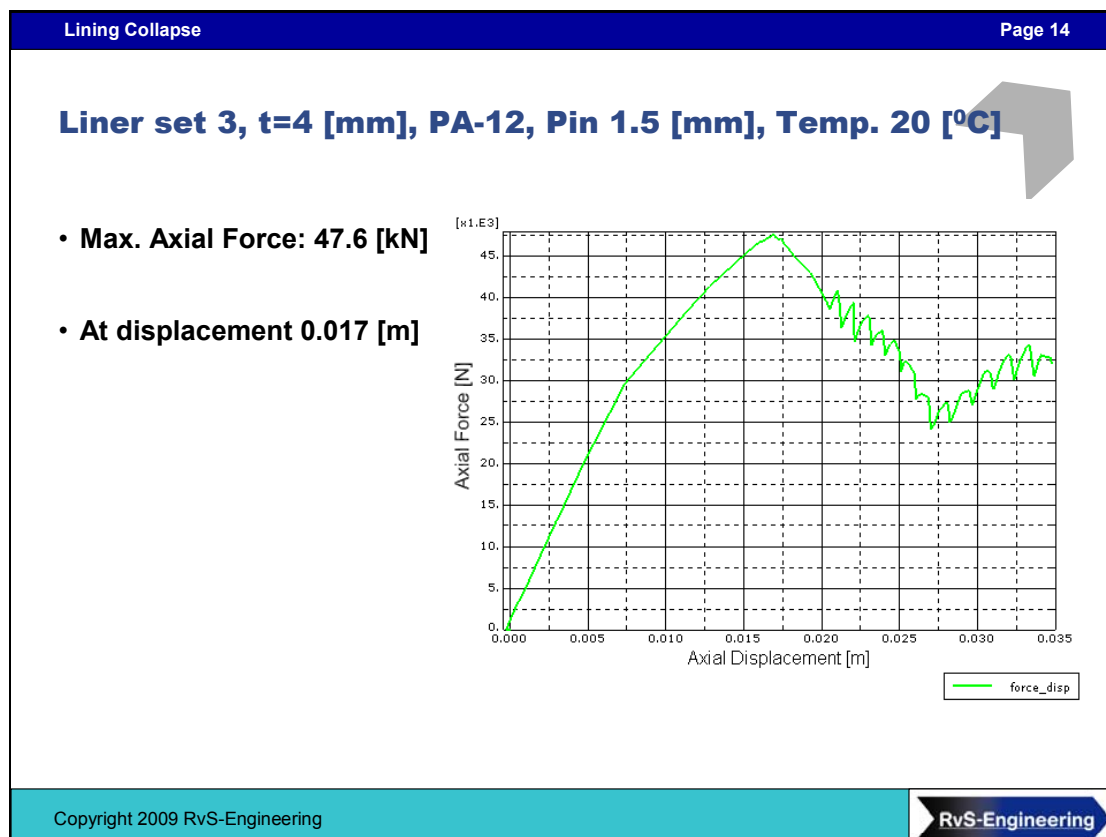
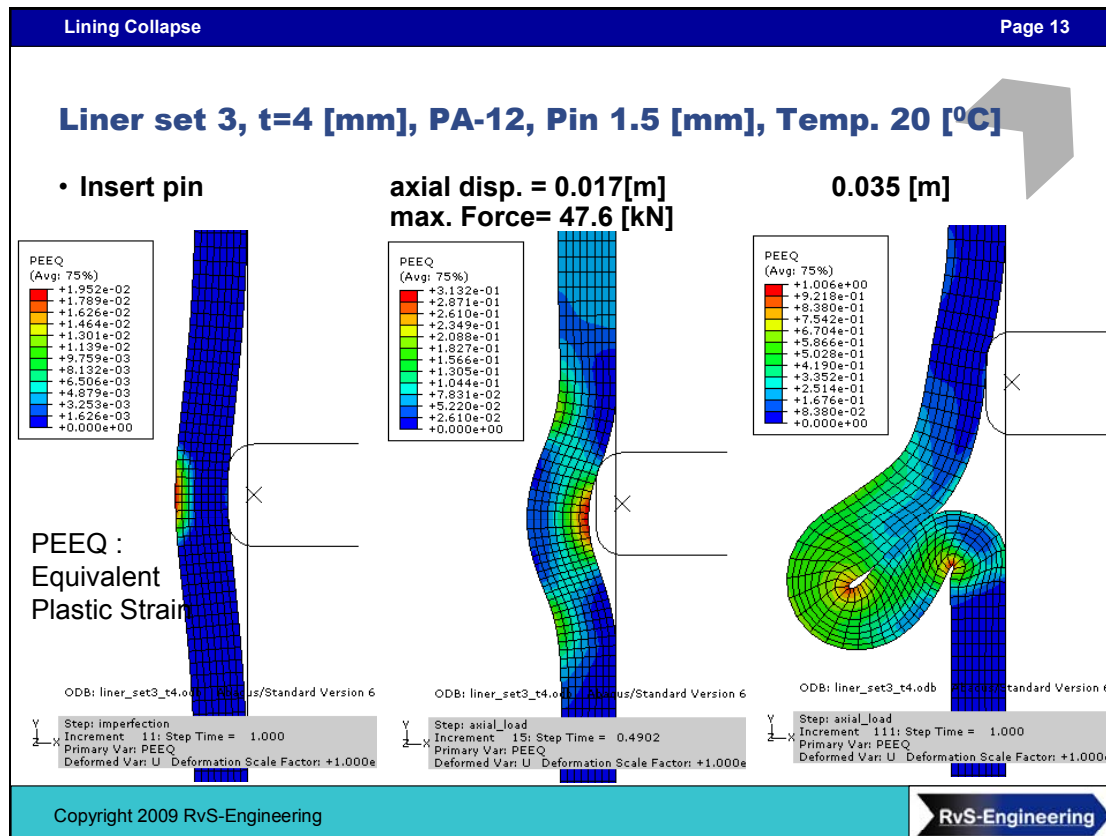


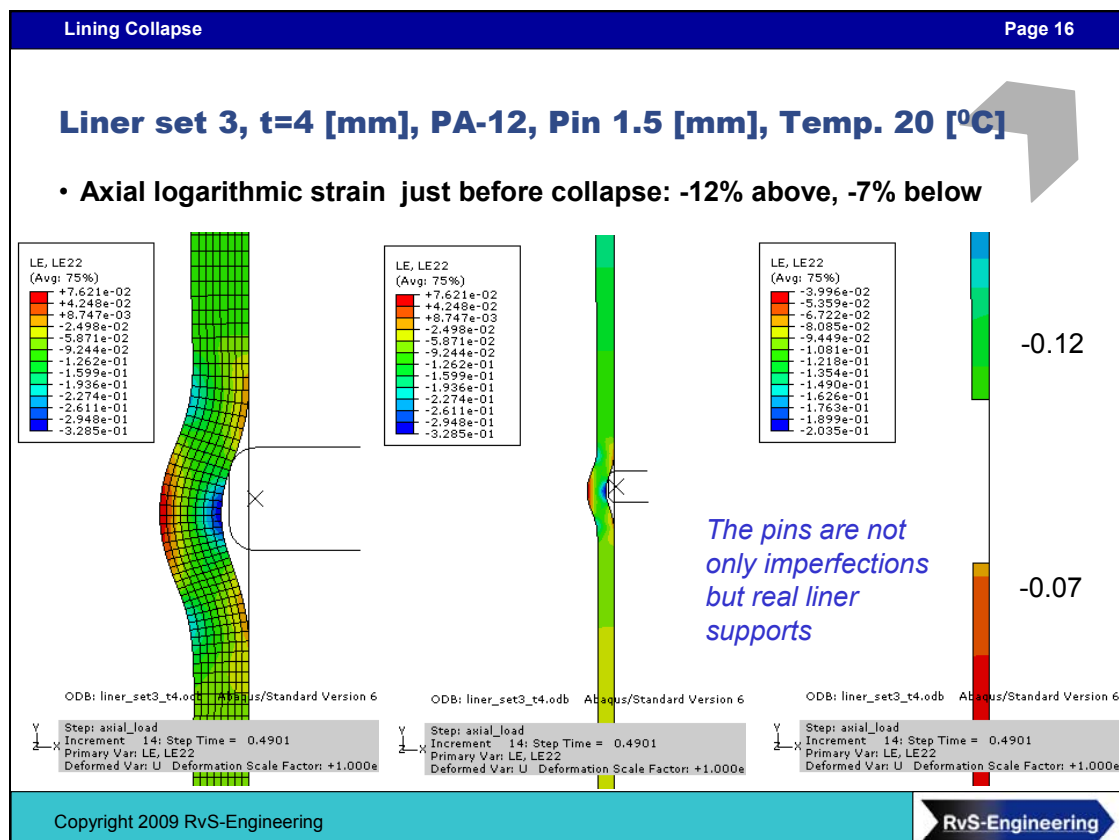
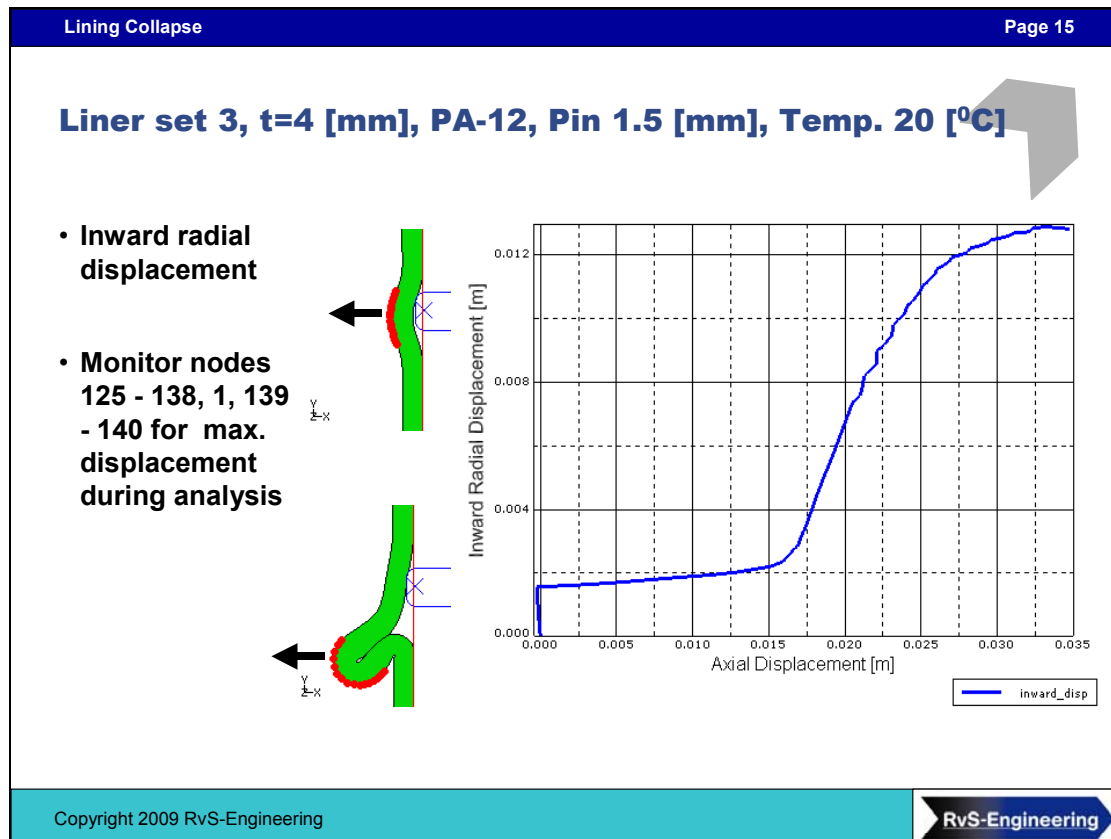
Liner set 3, $t=5$ [mm], PA-12, Pin 1.5 [mm], Temp. 20 [°C]

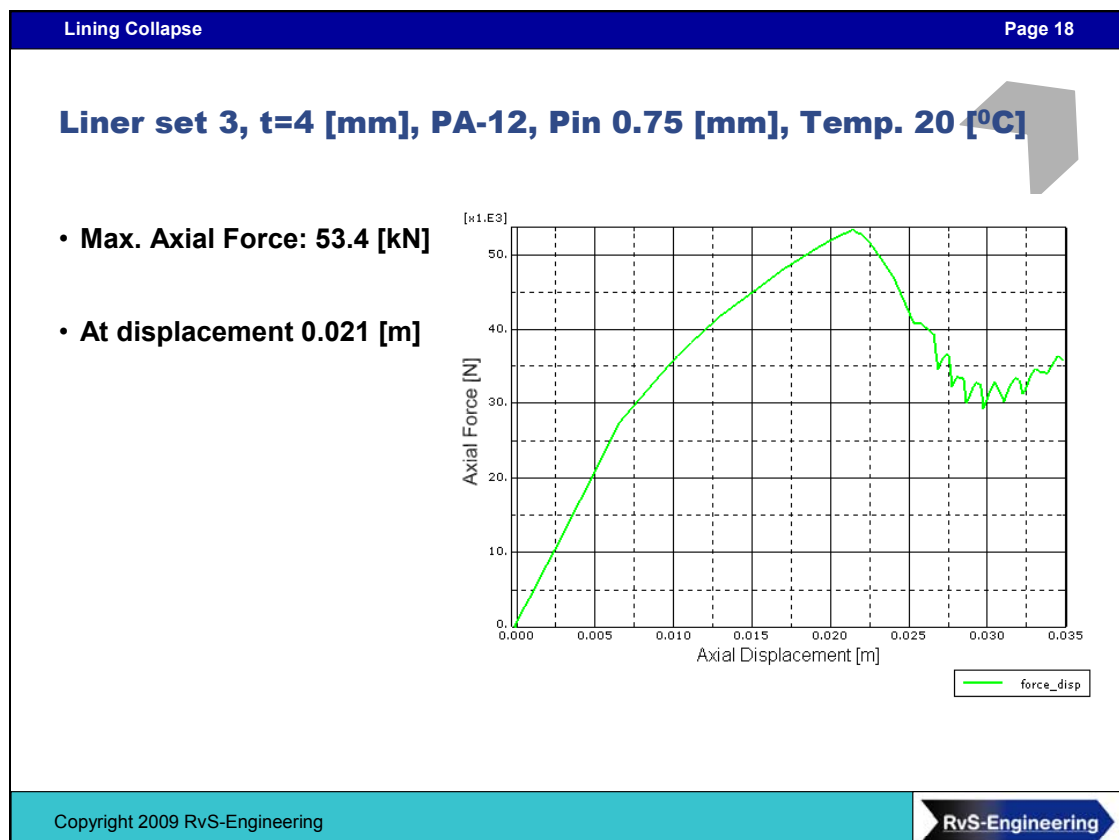
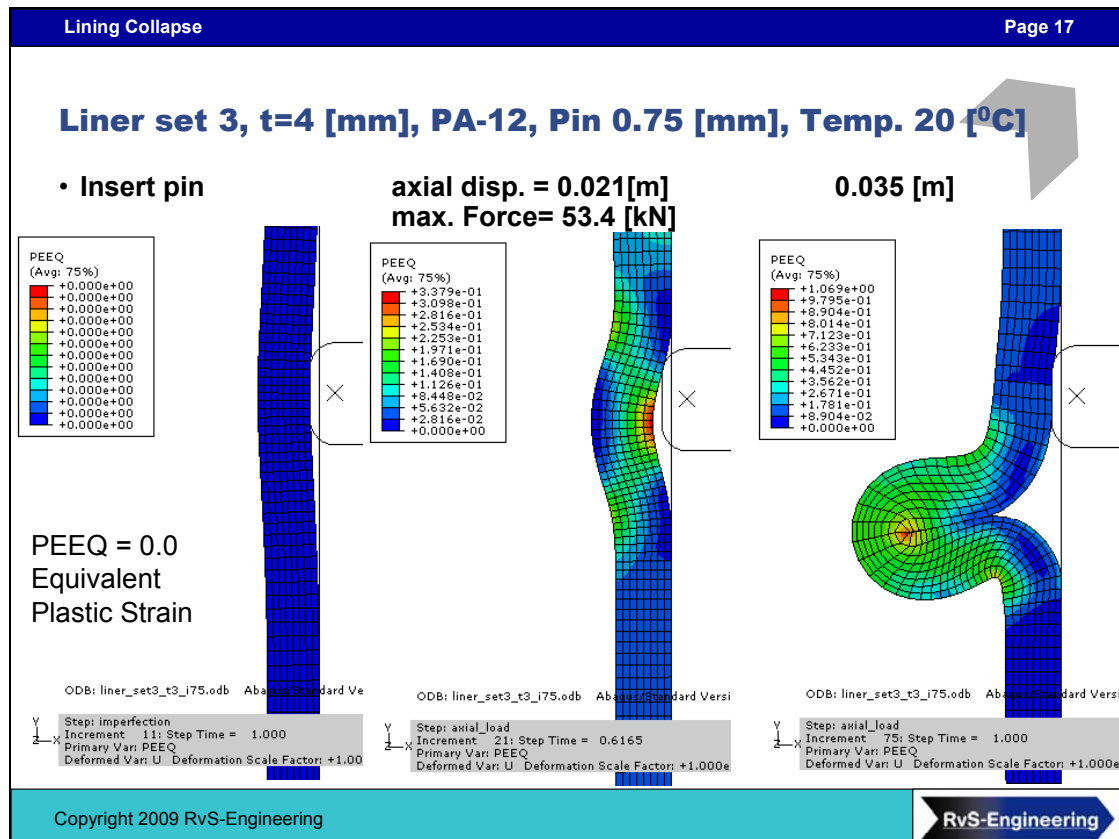
- Monitor node 129 at start not at center of imperfection
- When the collapse takes place 129 the best measuring point

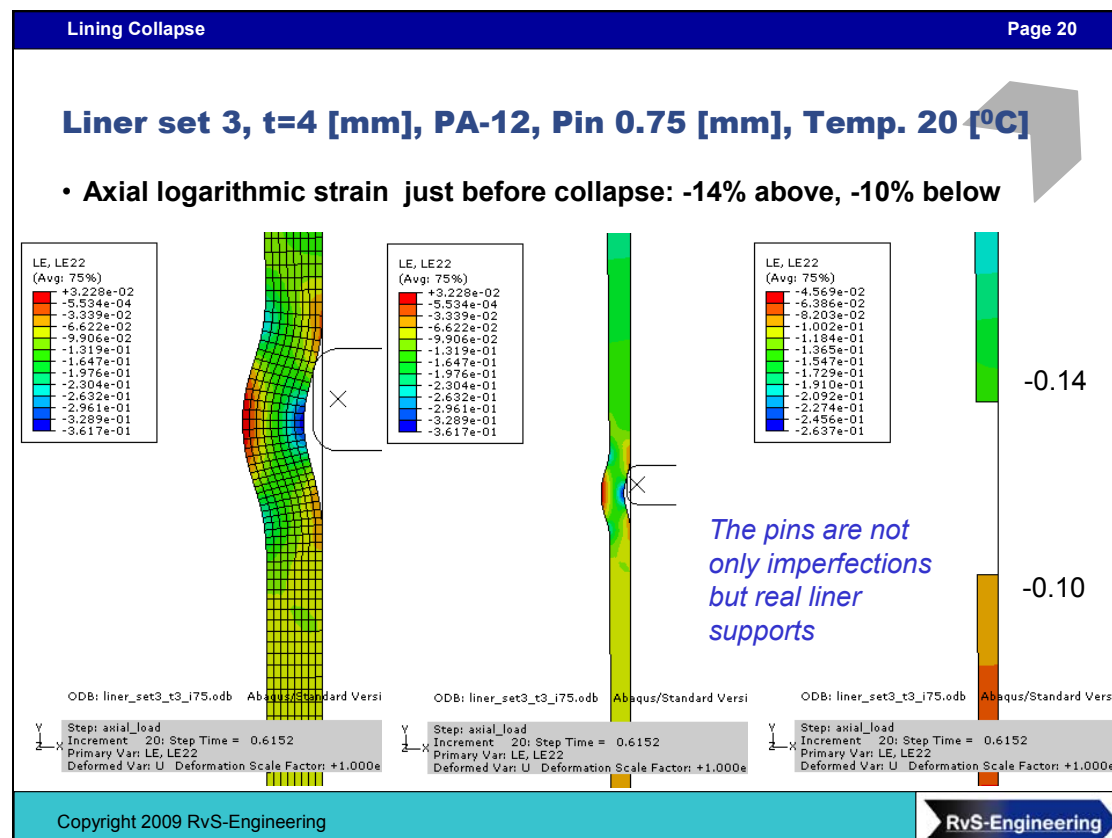
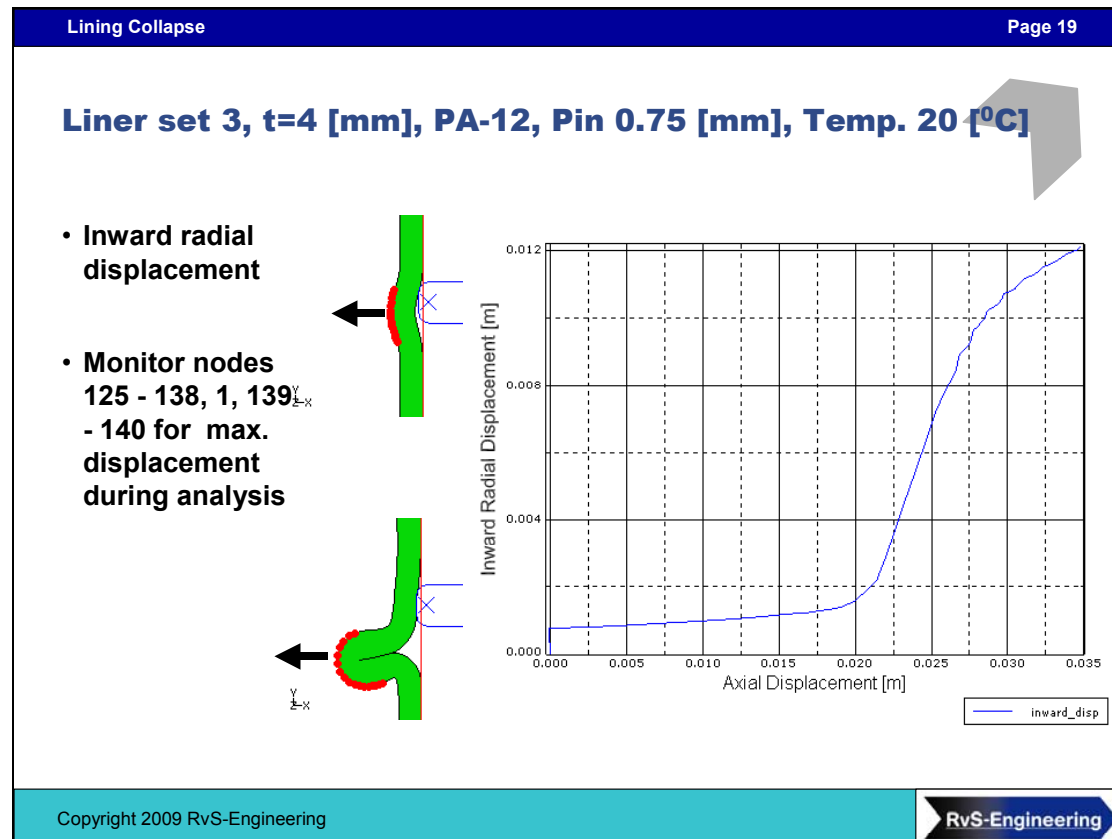


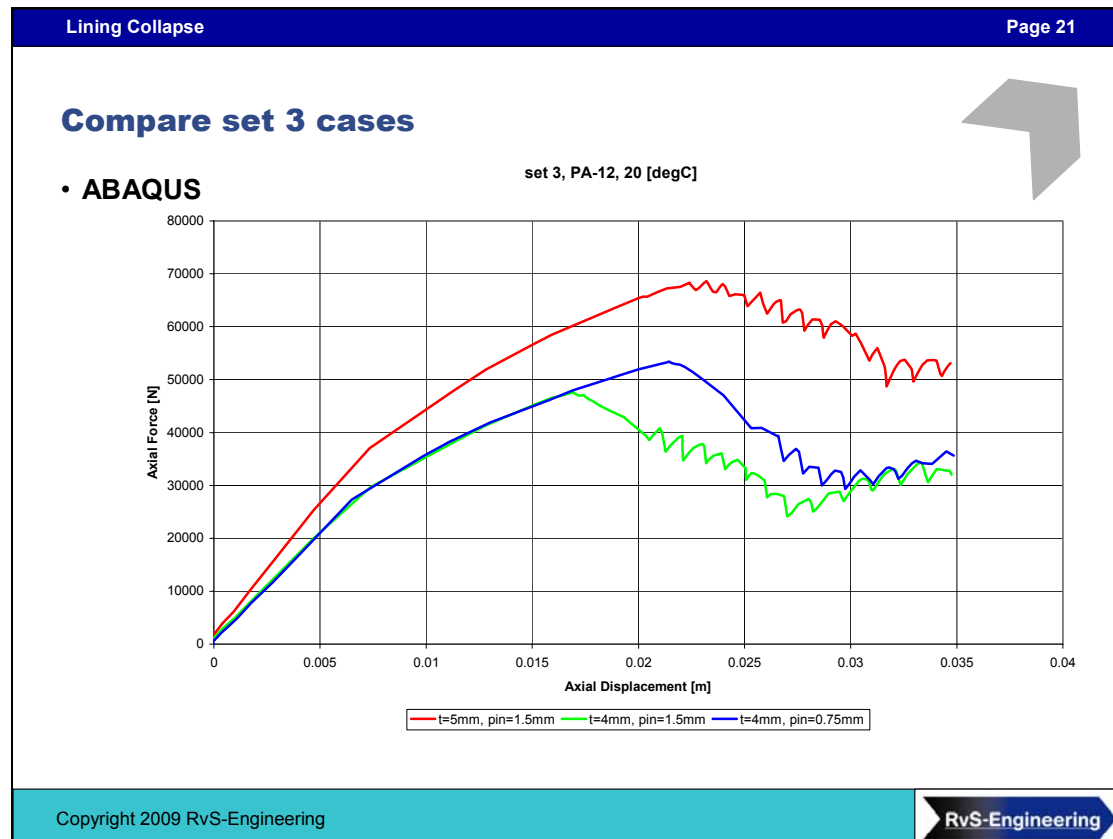












Lining Collapse

Page 22

RvS-Engineering

Shell GS Amsterdam

Axial Lining Collapse version 3

Ruben van Schalkwijk, 24 March 2009

Copyright 2009 RvS-Engineering

RvS-Engineering

Shell GS Amsterdam

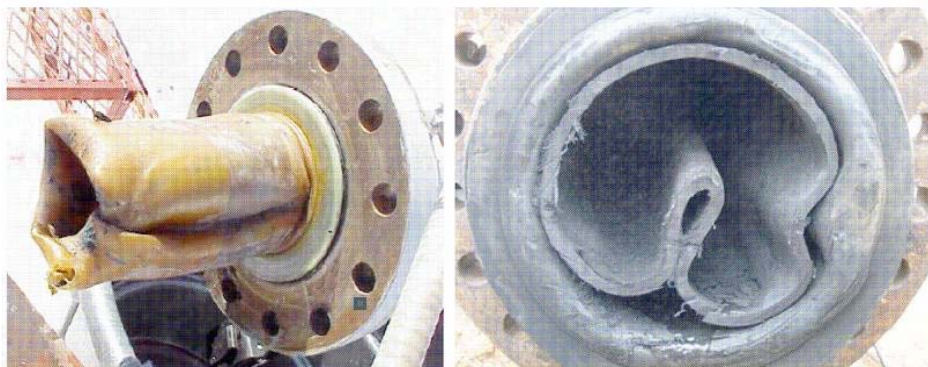
**Expansion Collapse 3D
version 1**

Ruben van Schalkwijk, March 2009

Copyright 2009 RvS-Engineering

Objective

- Model the mechanism behind liner failure



Example of an advanced stage axial buckling scenario of a PE liner.

Copyright 2009 RvS-Engineering

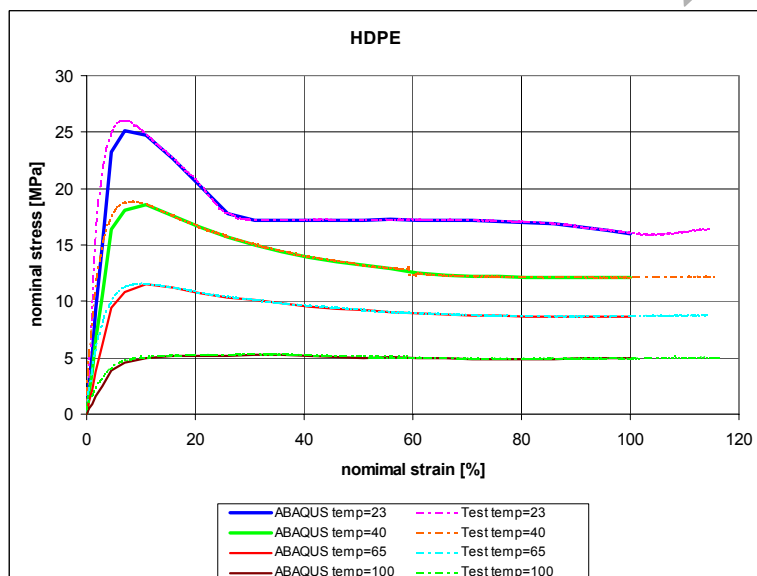
RvS-Engineering

Material Model HDPE

- Uni-axial HDPE material tensile test data are available for a range of temperatures
- A temperature dependent elasto-plastic model is used
- The elasticity and the true-yield stress versus true plastic strain is determined from the nominal stress versus nominal total strain test results
- To verify the results a simple tensile ABAQUS model is made to reproduce the test by simulation. See next slide.

Material Model HDPE

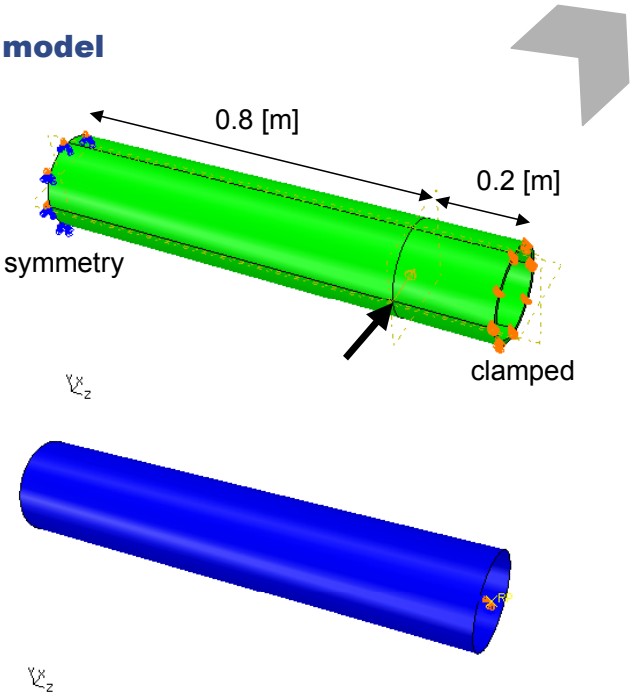
- Test-model
 - ABAQUS model
 - Experiment
- Thermal expansion coefficient $2.0 \cdot 10^{-4}$ [1/°C] in the whole temperature range



Lining CollapsePage 27

3D Expansion collapse model

- **Liner model**
 - OD=0.2 [m]
 - Thickness=0.01 [m]
- **Imperfection: point load**
- **Rigid pipe**



0.8 [m]

0.2 [m]

symmetry

clamped

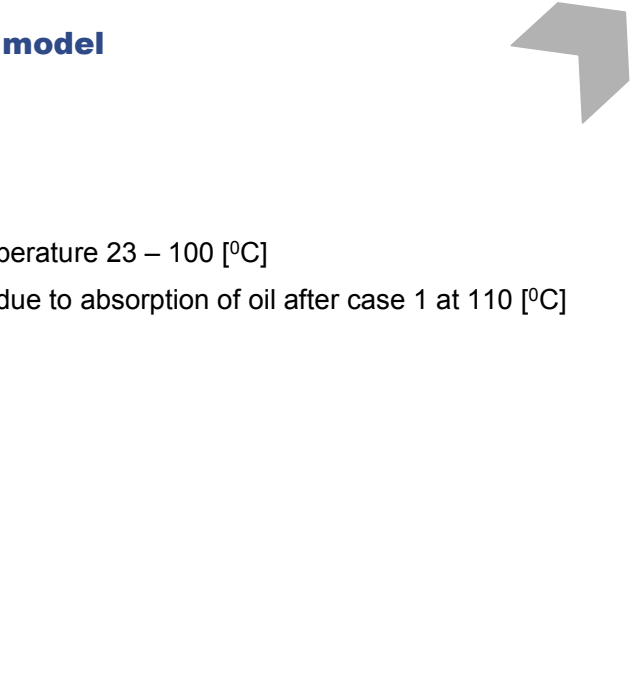
Copyright 2009 RvS-Engineering

RvS-Engineering

Lining CollapsePage 28

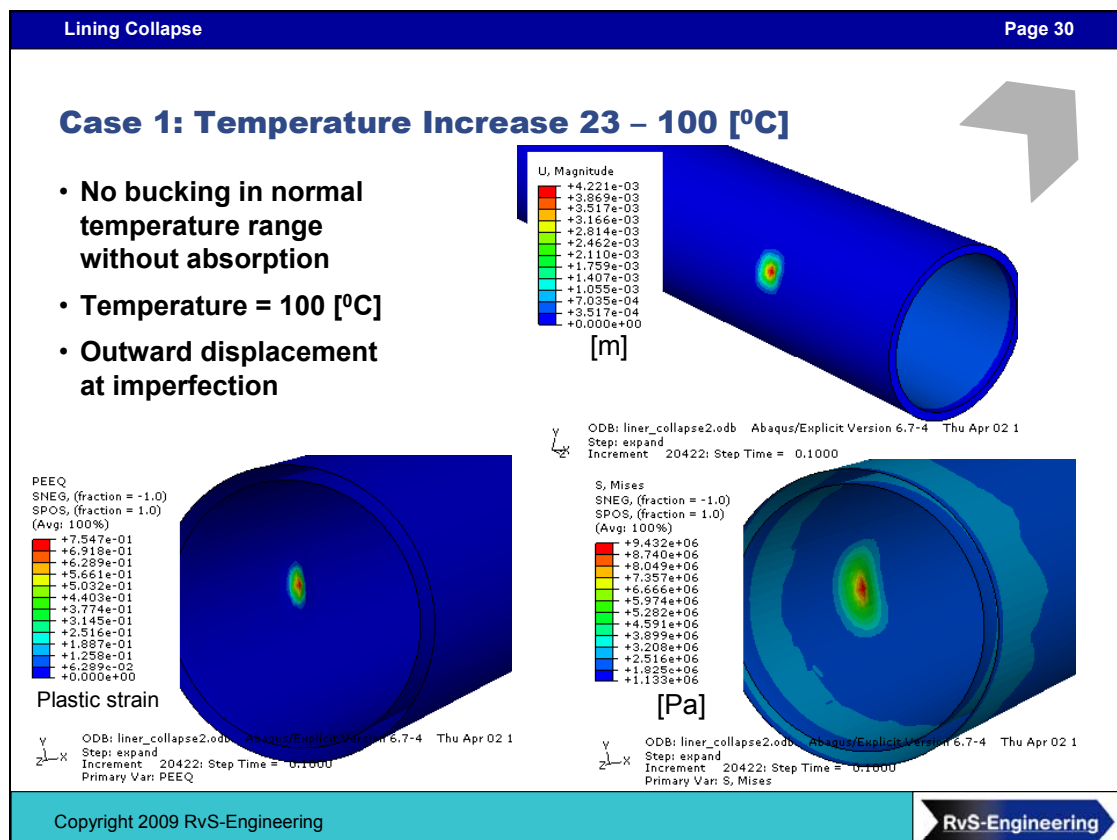
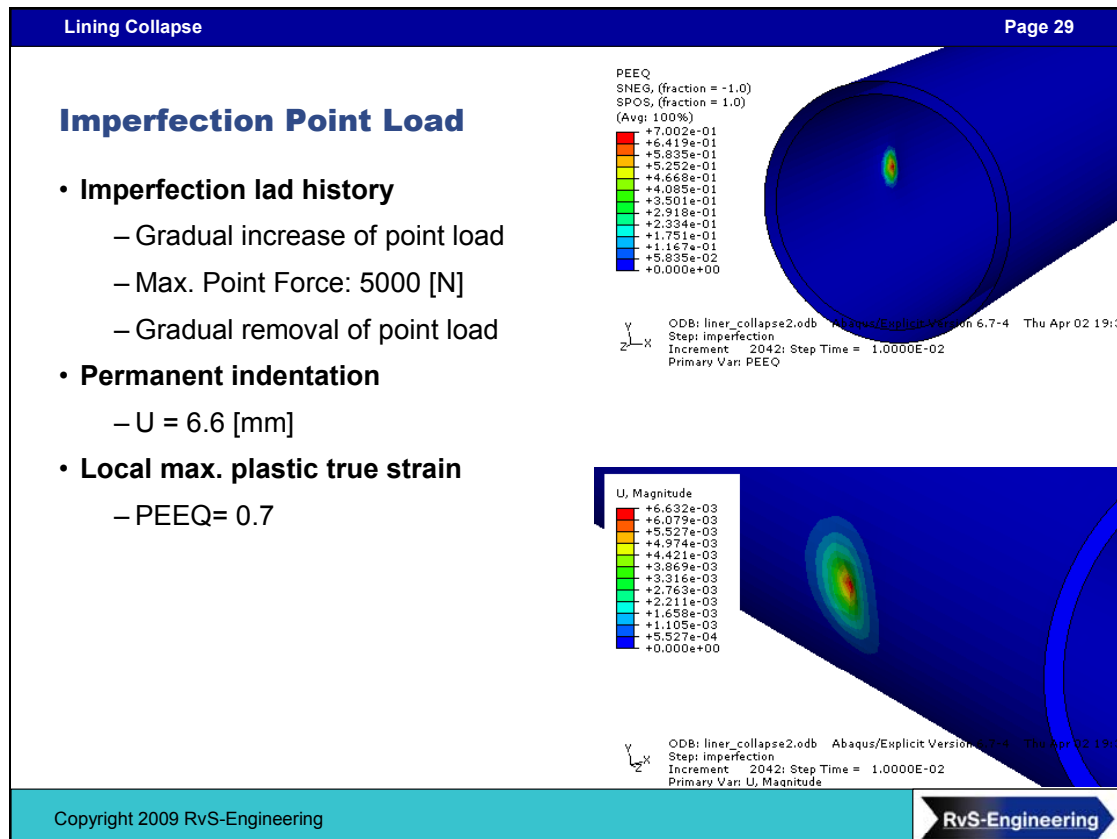
3D Expansion collapse model

- **Load history**
 - Initial temperature 23 [°C]
 - Imperfection: point load
 - Case 1: Increase the temperature 23 – 100 [°C]
 - Case 2: Extra expansion due to absorption of oil after case 1 at 110 [°C]
- **Contact interactions**
 - Liner to rigid pipe
 - Liner Self contact
 - Friction coefficient 0.1



Copyright 2009 RvS-Engineering

RvS-Engineering



Case 2: Absorption



- To get the liner to buckle the absorption of oil has to be modeled and
- The temperature must high (>100 [°C])
- The expansion coefficient is made dependent of a user defined field δ .
The total expansion strain can be calculated:

$$\alpha = 0.0002 + 0.9998 \cdot \delta$$

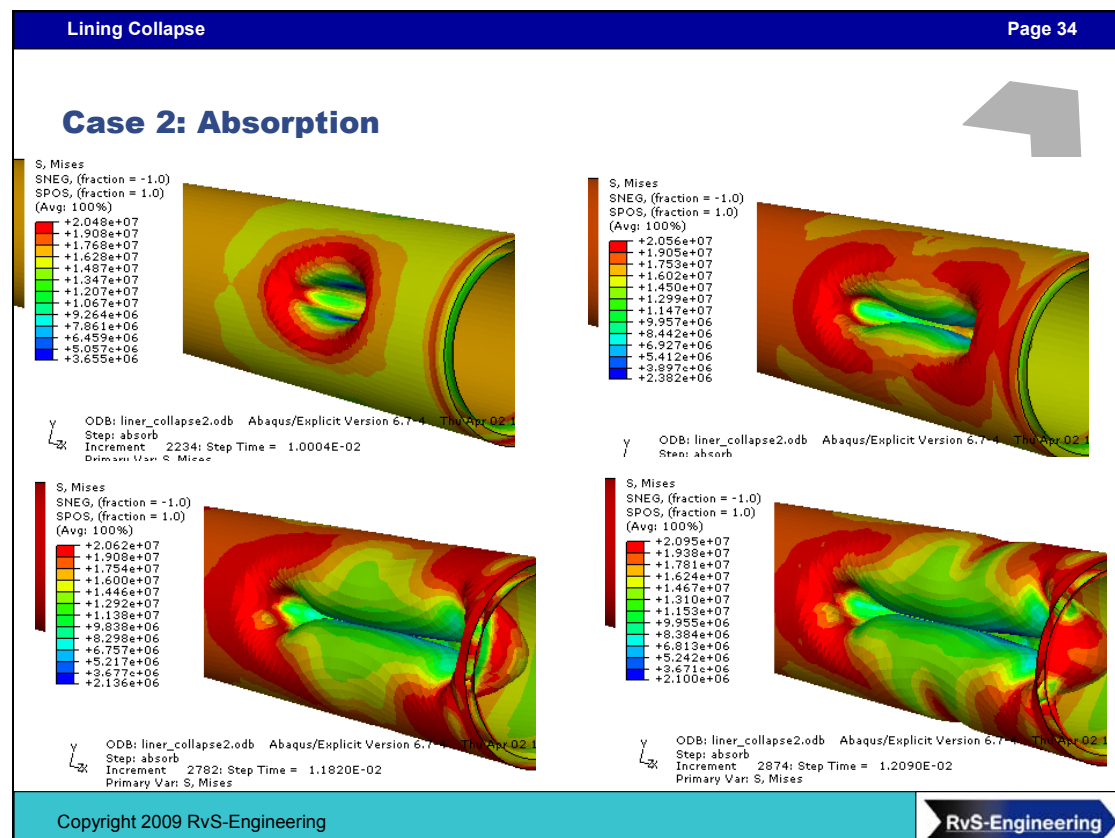
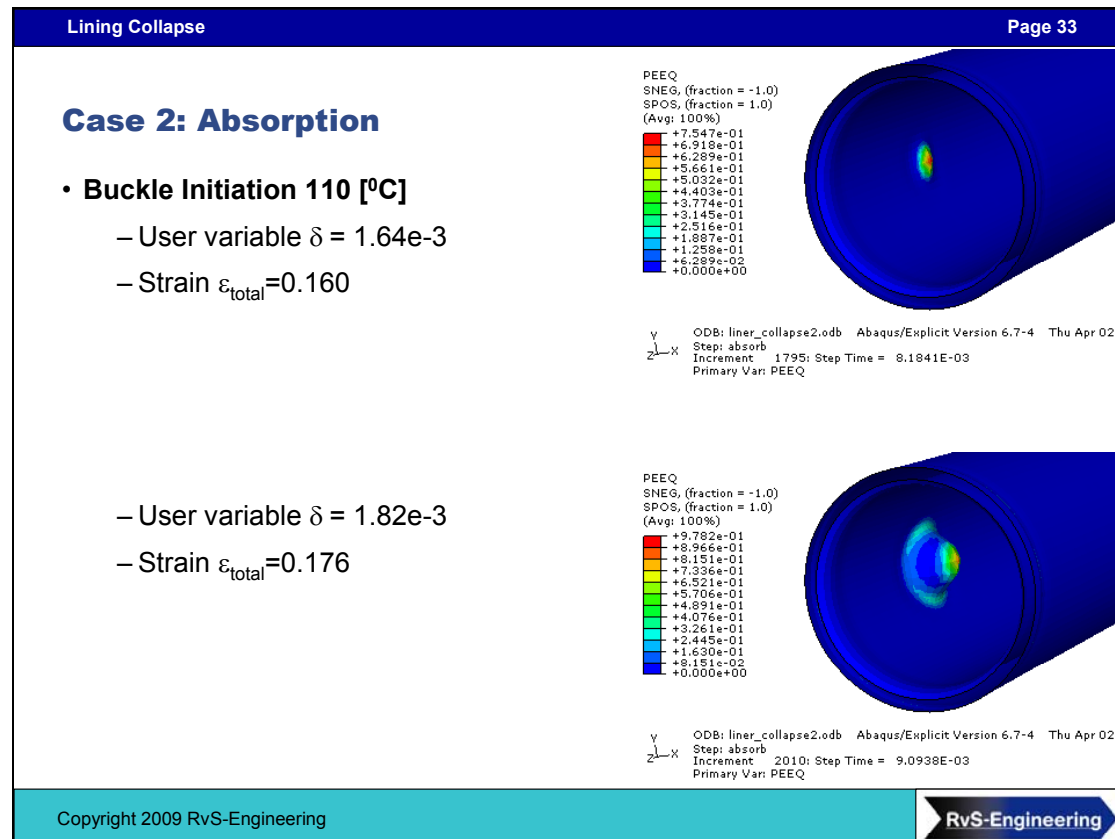
$$\varepsilon_{total} = \alpha \cdot (T - 23)$$

$$\frac{\Delta V}{V} = 3 \cdot \varepsilon_{total}$$

Case 2: Absorption



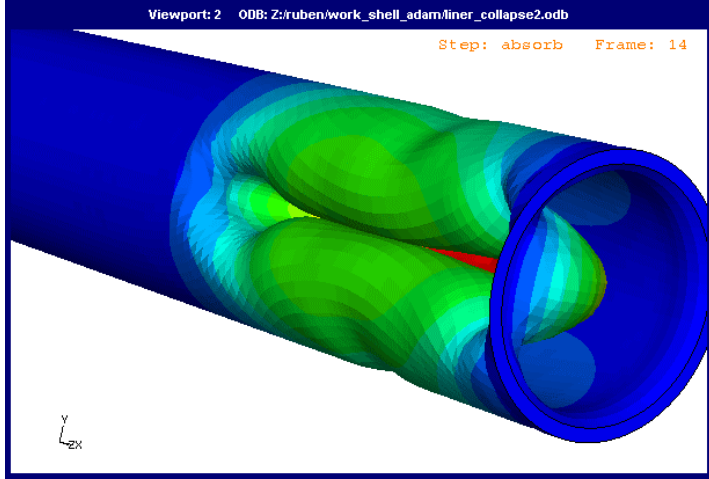
- Continue at 110 [°C] after case 1
- The high temperature and the absorbed oil changes the material and the elasto-plastic material model (slide 4) will not be valid anymore.
- The visco-elastic behavior should investigated and measured. The buckling deformation will be fast, therefore a elastic response is a reasonable guess. The modulus of elasticity is extrapolated to a smaller value:
– $E(110 [°C]) = 5.0e7 [Pa]$
- Shortly after the buckle, also for numerical reasons, the stress has to limited. Some relatively high plasticity have been introduced (yield=2.e7 [Pa], comparable with 40 [°C]).
- Better material model at higher temperatures and with absorbed oil has to be developed based on measurements



Lining CollapsePage 35

Case 2: Absorption

- Animation
- In full screen slide show



Copyright 2009 RvS-EngineeringRvS-Engineering

Lining CollapsePage 36



Shell GS Amsterdam

**Expansion Collapse 3D
version 1**

Ruben van Schalkwijk, March 2009

Copyright 2009 RvS-Engineering

Appendix B. Alternative approach for axial collapse equation based on maximum push load calculation method

Comparison with maximum push load calculation method provided in the Los Angeles City - Department of Public Works - Bureau of Engineering. Sewer design Manual.

The maximum push/pull force to be applied can be determined by the following formula.

$$P_{\max} = \sigma_{\max} \cdot A$$

P_{\max} : maximum push/pull force [N];

σ_{\max} : maximum allowable compressive stress [MPa];

A : cross sectional area, located at minimal cross section, of pipe [mm²].

From Roark⁶, axial compressive stress [MPa].

$$\sigma_{\max} = 0.3 \cdot E \cdot \frac{t}{r}$$

E : initial tensile or compressive modulus;

t : minimum wall thickness [mm];

r : mean radius [mm].

Combining the two equations gives:

$$P_{\max} = 0.3 \cdot E \cdot \frac{t}{r} \cdot A$$

$$\frac{P_{\max}}{E \cdot A} = 0.3 \cdot \frac{t}{r}$$

$$\varepsilon_{\max} = 0.3 \cdot 2 \cdot \left(\frac{1}{SDR - 1} \right)$$

In this format the equation is similar to the equation derived for axial buckling.

The value for n would be 1, the value for c would be 0.60.

In the SDR range of 10-40 value for $n=1$ and $c=0.6$ corresponds to IOD values of around 5.8 % for SDR 10 and 4.8 % for an SDR of 40.

⁶ Roark's Formulas for Stress and Strain.

Appendix C. Derivation of linear swell from volumetric swell

By L.M. de Mul - OGNL-GSEI/2

- (a) Assume a unit cell of polymer with dimensions $l \times l \times l$ (green cube).
- (b) Assume that the material swells homogeneous on exposure to a fluid, such that in all directions the swell will be $(l + dl)$ (red cube).

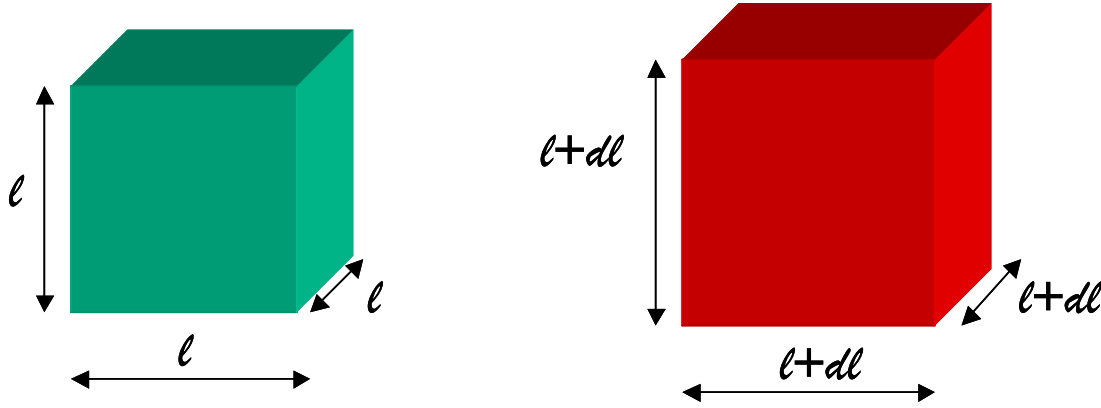


Figure C-1 Unit polymer cell before (green) and after (red) exposure to a fluid

The volume before and after exposure is:

$$V_{un\ exposed} = l^3 \quad (C-1)$$

$$V_{exposed} = (l + \delta l)^3 \quad (C-2)$$

Volumetric swell (fraction) is defined as:

$$\Delta V = \frac{(V_{exposed} - V_{un\ exposed})}{V_{un\ exposed}} \quad (C-3)$$

Substitution of Equations (C-1) and (C-2) into (C-3) gives:

$$\begin{aligned} \Delta V &= \frac{(l + \delta l)^3 - l^3}{l^3} \\ \Delta V &= \frac{(l + \delta l)^3}{l^3} - \frac{l^3}{l^3} \\ \Delta V &= \left(\frac{l + \delta l}{l} \right)^3 - 1 \\ \sqrt[3]{\Delta V + 1} &= \frac{l}{l} + \frac{dl}{l} \\ \sqrt[3]{\Delta V + 1} &= 1 + \varepsilon_{lin} \\ \varepsilon_{lin} &= \sqrt[3]{\Delta V + 1} - 1 \end{aligned} \quad (C-4)$$

The total axial strain is equal to the linear swell induced strain plus the thermal induced strain plus the hoop strain induced axial strain:

$$\varepsilon_{ax} = \varepsilon_{lin} + \varepsilon_{thermal} + \nu(\varepsilon_{lin} + \varepsilon_{thermal}) \quad (C-5)$$

The thermal induced strain is equal to:

$$\varepsilon_{thermal} = \alpha \cdot \Delta T \quad (C-6)$$

Substitution of Equations (4) and (6) into (5) gives:

$$\begin{aligned}\varepsilon_{ax} &= (\sqrt[3]{\Delta V + 1} - 1) + \alpha \cdot \Delta T + \nu \cdot \{ (\sqrt[3]{\Delta V + 1} - 1) + \alpha \cdot \Delta T \} \\ \varepsilon_{ax} &= (1 + \nu) \left\{ \sqrt[3]{\Delta V + 1} - 1 + \alpha \cdot \Delta T \right\}\end{aligned}\quad (\text{C-7})$$

With:

ΔV the volumetric swell (fraction)

ε_{ax} the axial strain (fraction)

or

$$\varepsilon_{ax} = (1 + \nu) \left\{ \sqrt[3]{\frac{\Delta V(\%)}{100} + 1} - 1 + \alpha \cdot \Delta T \right\}$$

With:

$\Delta V(\%)$ the volumetric swell in vol %

ε_{ax} the axial strain (fraction)

Appendix D. Data PA-12 (source Evonik-Degussa)

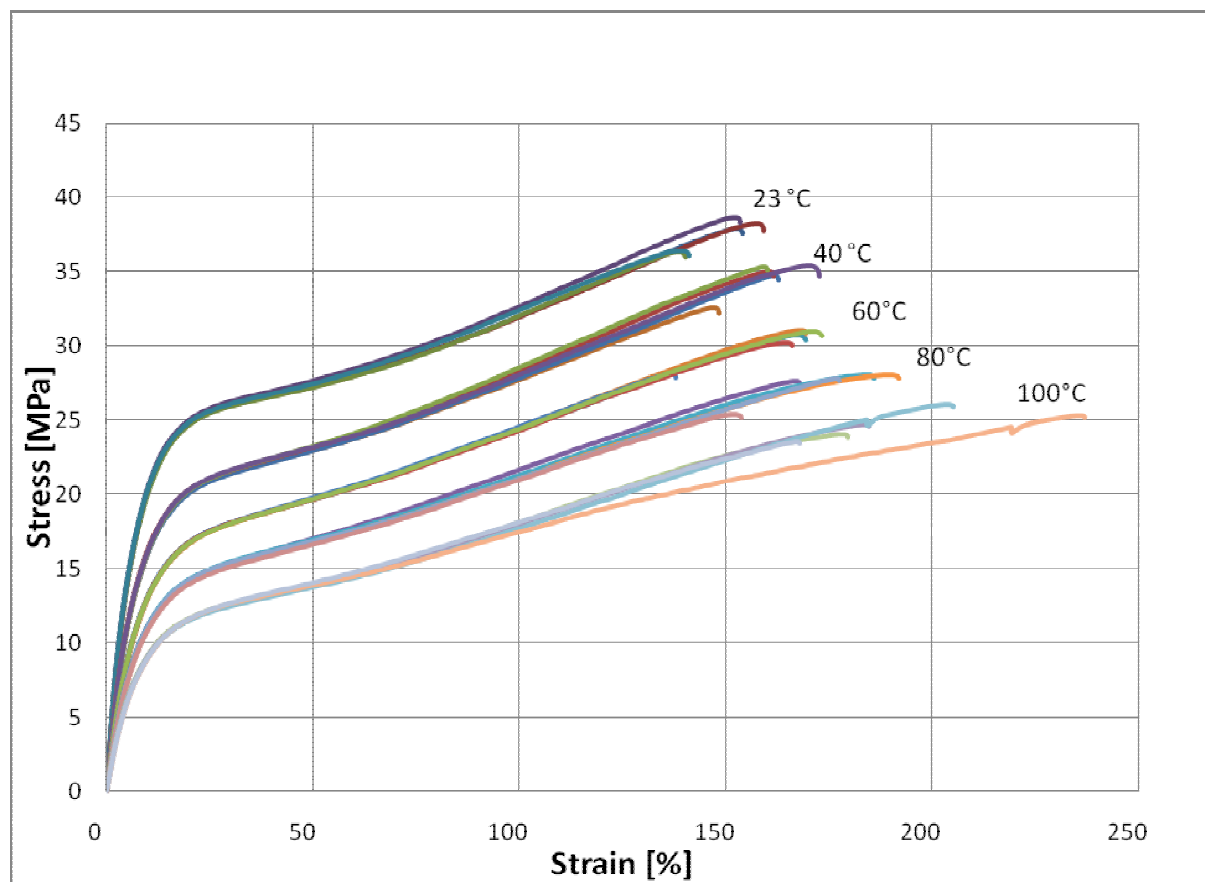


Figure D-1

Tensile curves Evonik-Degussa PA-12 LX9020, tested according to DIN-EN-ISO 527 at 23, 40, 60, 80 and 100 °C, $L = 115 \text{ mm}$, $L_0 = 50 \text{ mm}$, $v = 50 \text{ mm/min}$ (source : Evonik-Degussa)

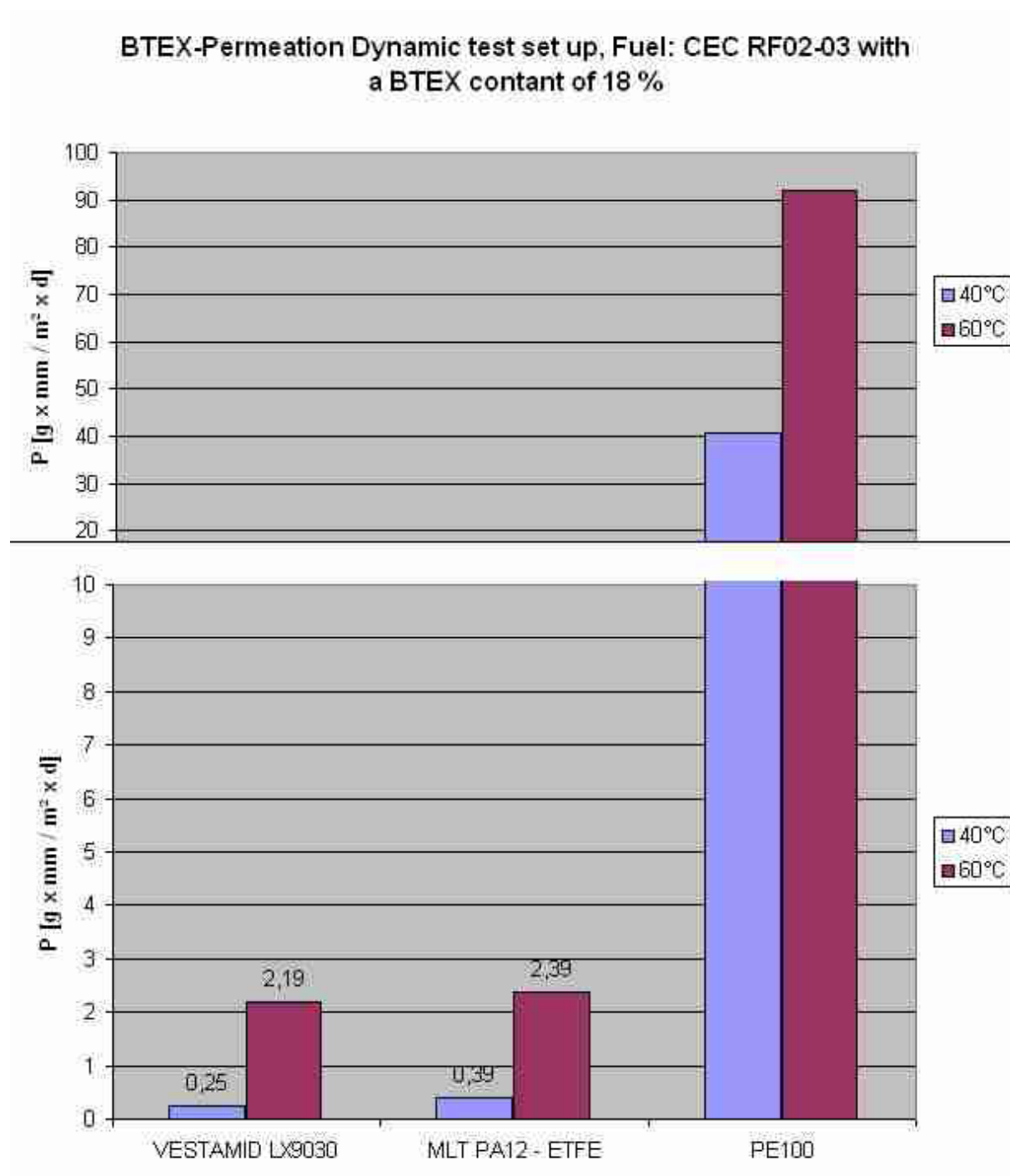
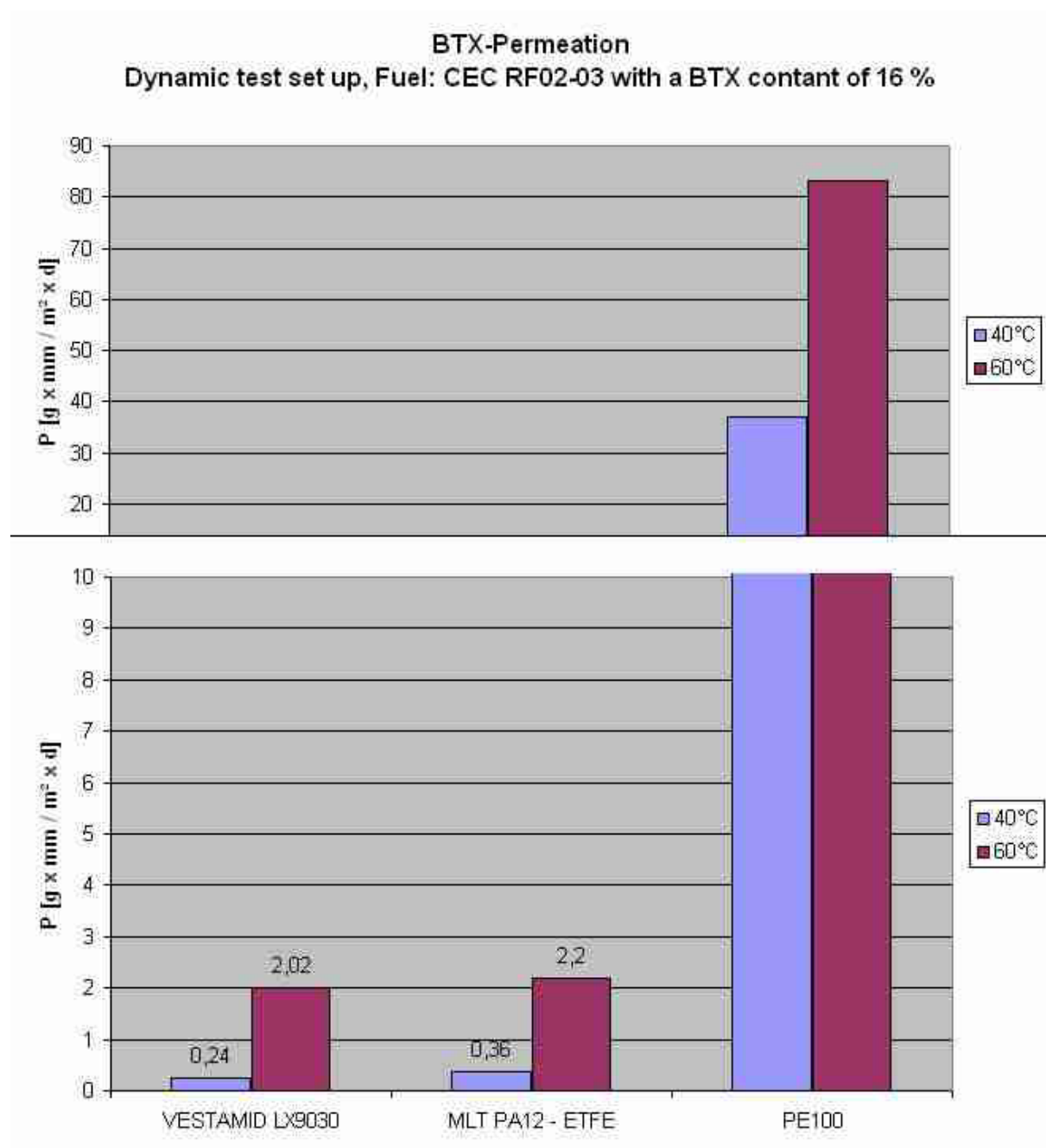


Figure D-2

BTEX permeation dynamic test set up, fuel: CEC RF02-03 with a BTX content of 18 %.
Exposure temperature 40 °C and 60 °C

**Figure D-3**

BTX permeation dynamic test set up, fuel: CEC RF02-03 with a BTX content of 16 %.
Exposure temperature 40 °C and 60 °C

Bibliographic information

This report has been classified as Restricted and is not subject to US Export Control regulations.

Report Number	: GS.09.54697	
Title	: Axial buckling design equation for thermoplastic lined carbon steel	
Author(s)	: L.M. de Mul	GSEI/2
Verified by	: F.A.H. Janssen	GSEI/2
Approved by	: B. McLoughlin	GSEI/2
Content Owner	: B. McLoughlin	GSEI/2
Issue Date	: December 2009	
Activity Code	: 54420373	
Sponsor	: Evonik Degussa GmbH	
Keywords	: HDPE, liner, pipeline, collapse, design	
Electronic file	: GS.09.54697.pdf	
Issuing Company	Shell Global Solutions International BV, Amsterdam P.O. Box 38000, 1030 BN Amsterdam, The Netherlands. Tel: +31 20 630 9111	

Customer Info

Name	: Evonik Degussa GmbH
Address	: Paul-Baumann Strasse 1 45772 Marl Germany

Shell Global Solutions International B.V. has its statutory seat in The Hague and its registered office at Carel van Bylandtlaan 30, 2596 HR, The Hague, the Netherlands. It is registered with the Chamber of Commerce in the Netherlands under number 27155370.

Report distribution

Outside Shell Global Solutions

Company name and address	E or P	No. of paper copies
Evonik Degussa GmbH, Marl C. Baron (christian.baron@evonik.com) A. Dowe (andreas.dowe@evonik.com) R. Tuellmann (ralf.tuellmann@evonik.com)	E E & P E	2
Shell Nederland Chemie B.V., Moerdijk F.J.M. Busch – CEI/2	E	

Within Shell Global Solutions

Name	Ref. ind.	Location	E or P	No. of paper copies
Shell Research and Technology Centre	GSNL-GSXI	(Reports Library) Amsterdam	E & P	1
J. Chang	GSUSI-GSEI/5	Houston	E	
F.A.H. Janssen	GSNL-GSEI/2	Amsterdam	E	
B. McLoughlin	GSNL-GSEI/2	Amsterdam	E	
L.M. de Mul	GSNL-GSEI/2	Amsterdam	E	
I. Ward	SCAN-GSEI/7	Calgary	E	

This report can be freely shared with all Shell Global Solutions employees.



Shell Global Solutions

For further information, contact Shell Global Solutions at:

Materials & Inspection Engineering

Shell Global Solutions International BV

P.O. Box 38 000, 1030 BN Amsterdam
The Netherlands

Tel: +31 (0) 20 630 3355

Fax: +31 (0) 20 630 2989

Email: Materials-Inspection@Shell.com

Web: www.shellglobalsolutions.com